## *Remarks*

Reconsideration of this Application is respectfully requested.

Claims 7-9, 14-16 and 35-40 are pending in the application, with claim 7 being the sole independent claim. Based on the following remarks, Applicants respectfully request that the Examiner reconsider all outstanding objections and rejections and that they be withdrawn.

### *I. "Office Action Summary" Page*

The Office Action Summary page of Paper No. 16 indicates that the Office Action is responsive to the communication filed on "22 October 2002." (*See* Paper No. 16, page 1, item 1.) Applicants' previous response, however, was filed on January 22, 2003. No communication was filed on October 22, 2002. A similar error was made on the Office Action Summary page of Paper No. 14, indicating that the Office Action was responsive to the communication filed on "09 May 2002." (*See* Paper No. 14, page 1, item 1.) The response that preceded Paper No. 14 was filed on August 8, 2002 and no communication was filed on May 9, 2002. Clarification is requested.

As the comments in the present Office Action appear to be directed to the remarks submitted in Applicants' previous response, Applicants assume that the present Office Action is intended to be responsive to the Amendment and Reply Under 37 C.F.R. § 1.111, filed on January 22, 2003.

## *II. Objection to the Specification*

The disclosure was objected to because, according to the Examiner, the status of the U.S. patent applications listed on pages 14 and 20-21 is missing. (*See* Paper No. 16, page 2.) Applicants respectfully request that this ground of objection be held in abeyance until the remaining issues in this application are resolved.

## *III. Claim Rejections Under 35 U.S.C. § 112, First Paragraph*

### *A. Written Description*

Claims 7, 9, 14, 16, 35 and 36 were rejected under 35 U.S.C. § 112, first paragraph, as allegedly containing subject matter which was not described in the specification in such a way as to reasonably convey to one skilled in the relevant art that the inventors, at the time the application was filed, had possession of the claimed invention. (*See* Paper No. 16, pages 2-3.) Applicants respectfully traverse this rejection.

This rejection is based on the assertion that "[t]he specification does not provide sufficient description of a genus of DNA molecules with 90% homology to SEQ ID NO: 1 that codes for a protein that has an activity of AD7c-NTP when over-expressed in neuronal cells." (Paper No. 16, pages 3-4.) For the reasons set forth in Applicants' previous responses, Applicants submit that the written description requirement is fully satisfied for the subject matter of claims 7, 9, 14, 16, 35 and 36. (*See* Applicants' Amendment and Reply Under 37 C.F.R. § 1.111, filed on January 22, 2003, (the "January 22, 2003 response") pages 6-9.)

To satisfy the written description requirement of 35 USC § 112, first paragraph, Applicants must convey with reasonable clarity to those skilled in the art that, as of the effective filing date, Applicants were in possession of the invention. *See Vas-Cath, Inc. v. Mahurkar*, 935 F.2d 1555, 1560, 19 USPQ2d 1111, 1117 (Fed. Cir. 1991). As made clear by the Federal Circuit, "[t]he written description requirement does not require the applicant 'to describe exactly the subject matter claimed, [instead] the description must clearly allow persons of ordinary skill in the art to recognize that [he or she] invented what is claimed.'" *Union Oil Co. of Cal. v. Atlantic Richfield Co.*, 208 F.3d 989,997, 54 USPQ2d 1227, 1232 (Fed. Cir. 2000). In addition, not all functional descriptions of genetic material necessarily fail to meet the written description requirement; rather, "the requirement may be satisfied if in the knowledge of the art the disclosed function is sufficiently correlated to a particular, known structure." *Enzo Biochem, Inc. v. Gen-Probe Inc.*, 296 F.3d 1316, 1324 (Fed. Cir. 2002); *See also, Moba, B.V. v. Diamond Automation, Inc.*, 2003 U.S. App. LEXIS 6285 at 31-32 (Fed. Cir. 2003).

A person of ordinary skill in the art would have recognized that Applicants, at the time the application was filed, were in possession of the invention insofar as it encompasses transgenic non-human animals whose germ and somatic cells comprise a DNA molecule of SEQ ID NO: 1 or a DNA molecule which is at least 90% homologous thereto, wherein said DNA molecule is over-expressed in one or more cells of said transgenic animal, and wherein said DNA molecule codes for a protein that has an activity of AD7c-NTP when over-expressed in neuronal cells.

First, the DNA molecules included within the germ and somatic cells of the claimed transgenic animals are not defined *solely* in terms of their function. As specified in claim

7, the germ and somatic cells of the transgenic animals comprise the DNA molecule *of SEQ ID NO: 1* or a DNA molecule *which is at least 90% homologous thereto*. Thus, the claims include a structural definition of the DNA constructs.

Second, procedures for isolating nucleic acid molecules that are at least 90% homologous to SEQ ID NO:1 are described in the specification and were well-known in the art. (*See, e.g.*, specification at page 19, lines 3-15.) Moreover, assays are described in the specification for determining whether a DNA molecule encodes a protein having an activity of AD7c-NTP when over-expressed in neuronal cells. (*See* specification at page 20, lines 1-29, and at page 45, line 16 through page 46, line 26.)

The detail provided in the specification for obtaining DNA molecules that are at least 90% homologous to SEQ ID NO: 1 and for determining whether they encode proteins having an activity of AD7c-NTP when overexpressed in neuronal cells would indicate to persons of ordinary skill in the art that Applicants were in possession of DNA molecules having the nucleotide sequence of SEQ ID NO: 1 and DNA molecules having a nucleotide sequence that is at least 90% identical to SEQ ID NO: 1. By extension, persons of ordinary skill in the art would have recognized that Applicants had invented transgenic animals whose germ and somatic cells comprise the DNA molecule of SEQ ID NO: 1 or a DNA molecule that is at least 90% homologous thereto. This conclusion is fully supported by the USPTO's "Synopsis of Application of Written Description Guidelines" and by the Federal Circuit's current interpretation and application of 35 U.S.C. § 112, first paragraph. (*See* Applicants' remarks set forth in the Amendment and Reply filed on August 8, 2002, ("the August 8, 2002 response") pages 8-12.) Applicants therefore respectfully request that the

written description rejection of claims 7, 9, 14, 16, 35 and 36 be reconsidered and withdrawn.

***B. Enablement***

Claims 7-9, 14-16 and 35-40 were rejected under 35 U.S.C. § 112, first paragraph, as allegedly containing subject matter which was not described in the specification in such a way as to enable one skilled in the art to which it pertains, or with which it is most nearly connected to make and/or use the invention. (*See* Paper No. 16, page 6.) Applicants respectfully traverse this rejection.

In order to satisfy the enablement requirement of 35 USC § 112, first paragraph, the claimed invention must be enabled so that any person skilled in the art can make and use the invention without undue experimentation. *See In re Wands*, 858 F.2d 731, 737, 8 USPQ2d 1400, 1404 (Fed. Cir. 1988). Since it would require only routine experimentation for a person of ordinary skill in the art to make and use the transgenic non-human animals of claims 7-9, 35, 36, 39 and 40 and to practice the methods of claims 14-16, 37 and 38, the enablement requirement of 35 U.S.C. § 112, first paragraph, is fully satisfied.

***1. Enablement Provided for the DNA Molecules That are Included Within the Transgenic Animals of the Invention***

The rejection is based, in part, on the assertion that it would have required undue experimentation for a skilled artisan to obtain a DNA molecule that is at least 90% homologous to SEQ ID NO:1 and that codes for a protein that has an activity of AD7c-NTP when over-expressed in neuronal cells. (*See* Paper No. 16, pages 7-8.) As explained in Applicants' previous response, a person of ordinary skill in the art, using only routine

methods, would have been able to obtain the DNA molecules that are used to produce the transgenic animals of the invention. (*See* the January 22, 2003 response, pages 10-11.)

The specification provides exemplary methods for obtaining DNA molecules which are at least 90% homologous to SEQ ID NO:1. Such methods involve, *e.g.*, the isolation of DNA molecules from cDNA libraries by hybridization under stringent conditions to the DNA molecule of SEQ ID NO:1. (*See* specification at page 19, lines 3-15.) Additional methods for obtaining DNA molecules that are at least 90% homologous to SEQ ID NO:1 include the use of directed and random mutagenesis techniques. Such methods were well known to those of ordinary skill in the art at the time of the invention. *See, e.g.*, Sambrook *et al.*, "Creating Many Mutations in a Defined Segment of DNA," in *Molecular Cloning, A Laboratory Manual*, Sambrook *et al.*, eds., Cold Spring Harbor Laboratory Press, pp. 15.95-15.108 (1989) (copy attached to the January 22, 2003 response, as Exhibit 1).

Once obtained, DNA molecules that are at least 90% homologous to SEQ ID NO:1 could have easily been tested for the ability to encode a protein having an activity of AD7c-NTP. The specification describes various methods for assaying for AD7c-NTP activity. For example, transgenic animals can be made that over-express AD7c-NTP in neuronal cells, and, once obtained, the transgenic animals may be analyzed for evidence of neuronal or neuritic abnormalities associated with Alzheimer's disease, neuroectodermal tumors, malignant astrocytomas and glioblastomas. (*See* specification at page 20, lines 1-29.)

Additionally, *in vitro* methods could have been used to test for AD7c-NTP activity. For example, the specification exemplifies an assay involving the overexpression of AD7c-NTP in neuronal cells and the subsequent analysis for cellular characteristics of Alzheimer's disease, including apoptosis and neuritic sprouting. (*See* specification at page 46, lines 4-

26.) Thus, the full range of DNA molecules that are included within the transgenic animals of the invention could have been easily made and analyzed by persons of ordinary skill in the art using only routine methods and experimentation.

The Examiner cited *Amgen, Inc. v. Chugai Pharmaceutical Co., Ltd.*, 927 F.2d 1200 (Fed. Cir. 1991) to support the enablement rejection. (*See* Paper No. 16, page 8). The claims at issue in *Amgen*, however, were directed to DNA sequences defined solely in functional terms.[1] The present claims specify that the germ and somatic cells of the transgenic animals comprise the DNA molecule of SEQ ID NO:1 or a DNA molecule which is at least 90% homologous thereto, and wherein the DNA molecule codes for a protein that has an activity of AD7c-NTP when over-expressed in neuronal cells. Therefore, the reasoning set forth in *Amgen* for finding the claims non-enabled cannot be used to support a rejection of the present claims for lack of enablement.

### *2. Enablement Provided for the Transgenic Animals That are Encompassed by or Used in the Practice of the Claimed Invention*

The rejection is also based on the assertion that:

> the as-filed specification does not provide sufficient guidance or factual evidence for using the DNA molecule for making a transgenic non-human animal expressing a nucleotide sequence encoding SEQ ID NO: 1 or a DNA molecule, which is at least 90% homologous thereto, and any corresponding phenotype.

---

[1]Claim 7 of U.S. Patent No. 4,703,008, the claim at issue in the enablement analysis of *Amgen*, is as follows: "A purified and isolated DNA sequence consisting essentially of a DNA sequence encoding a polypeptide having an amino acid sequence sufficiently duplicative of that of erythropoietin to allow possession of the biological property of causing bone marrow cells to increase production of reticulocytes and red blood cells, and to increase hemoglobin synthesis or iron uptake." *Amgen* at 1204.

(Paper No. 16, page 9.) Applicants respectfully disagree. As stated in the previous response, methods for creating transgenic animals encompassed by and used in the practice of the claimed invention would have required no more than routine experimentation. (*See* the January 22, 2003 response, pages 12-15.)

The rejection is based to a large extent on the interpretation of the claims as requiring that the transgenic animals "[express] the protein at a level sufficient to result in a specific phenotype." (Paper No. 16, page 11.) The Examiner stated that:

> [w]hile the state of the art of transgenics is such that one of skill in the art would be able to produce [a] transgenic animal comprising a transgene of interest (e.g. SEQ ID NO: 1 or a sequence with 90% homology thereto); it is not predictable if the transgene would be expressed at a level and specificity sufficient to cause a particular phenotype.

(Paper No. 16, page 11.) Applicants respectfully disagree with the Examiner's interpretation of the claims.

As noted in the January 22, 2003 response, none of the claims, except for claims 37 and 38, specify a phenotype exhibited by the transgenic animals. (*See* the January 22, 2003 response, pages 26-27.) The specification does not indicate that the claims should be interpreted to require that the transgenic animals exhibit any specific phenotype.

The Examiner stated that "it is unknown what other purpose the transgenic animal would serve if the transgene (e.g. AD7c-NTP) is not expressed at a sufficient level for a resulting phenotype." (Paper No. 16, page 17.) As previously asserted, transgenic animals encompassed by or included within the subject matter of claims 7-9, 14-16, 35, 36, 39 and 40 are useful in, *e.g.*, drug screening applications even if they do not exhibit any specific phenotypes. (*See* January 22, 2003 response, pages 26-27.) The Examiner nonetheless stated that:

> it is not apparent to one skilled in the art how a transgenic non-human animal can be used in an assay for screening a candidate drug of Alzheimer's disease, neuroectodermal tumors, malignant astrocy[t]omas, and glioblastomas in a transgenic non-human animal comprising a nucleotide sequence that is SEQ ID NO: 1 or 90% homologous to SEQ ID NO: 1, if a phenotype comprising neuritic sprouting, nerve cell death, nerve cell degeneration, neurofibrillary tangles, and/or irregular swollen neurites in neuronal cells is not observed in the transgenic animal.

(Paper No. 16, page 17.) The use of transgenic animals of the invention for drug screening applications, wherein the animals *do not* exhibit neuritic sprouting, nerve cell death, nerve cell degeneration, neurofibrillary tangles, and/or irregular swollen neurites, was set forth in the previous response. (*See* the January 22, 2003 response, page 27.)

Briefly, candidate drugs can be administered to a transgenic animal whose germ and somatic cells comprise the DNA molecule of SEQ ID NO:1 or a DNA molecule which is at least 90% homologous thereto. Candidate drugs can be identified by their ability to cause, *e.g.*, the suppression or prevention of expression of the protein encoded by the DNA molecule contained by the transgenic animal. (*See* specification at page 21, line 12.) Alternatively, drugs can be identified on the basis of their ability to increase the degradation of the protein encoded by the DNA molecule contained by the transgenic animal. (*See* specification at page 21, line 13.) Method claims 14-16 specifically comprise detecting at least one of the following: (i) the suppression or prevention of expression of the protein coded for by the DNA molecule contained by said animal; or (ii) the increased degradation of the protein coded for by the DNA construct contained by said animal. The only characteristic that the transgenic animals encompassed by or included within the subject matter of claims 7-9, 14-16, 35, 36, 39 and 40 need to possess in order to be useful for the contemplated screening methods is that they express the DNA molecule of SEQ ID NO:1

or a DNA molecule that is at least 90% homologous thereto. It is unnecessary that they exhibit neuritic sprouting, nerve cell death, nerve cell degeneration, neurofibrillary tangles, and/or irregular swollen neurites.

Notwithstanding the fact that none of the claims, except claims 37 and 38, specify a phenotype exhibited by the transgenic animals, Applicants respectfully disagree with the assertion that the production of transgenic animals of the invention that exhibit a specific phenotype (*e.g.*, neuritic sprouting, nerve cell death, nerve cell degeneration, neurofibrillary tangles, and/or irregular swollen neurites) would have required undue experimentation.

The Examiner cited Polejaeva *et al.*, *Theriogenology 53*:117-126 (2000) to show that "producing transgenic animals with a predictable phenotype was considered unpredictable." (Paper No. 16, page 9.) As previously noted, Polejaeva discusses the successful production of many species of transgenic animals and therefore does not suggest that transgenic animal production would have required undue experimentation. (*See* the January 22, 2003 response at pages 21-24.)

The Examiner also asserted various technical issues relating to the production of transgenic animals, including "[t]he individual gene of interest, coding, or non-coding sequences present in the transgene construct, [and] the specificity of transgene integration into the genome." (Paper No. 16, page 12.) In addition, the Examiner cited Wall, R.J., *Theriogenology 45*:57-68 (1996), Houdebine, L-M., *J. Biotechnology 34*:269-287 (1994), Mullins, L.J. and Mullins, J.J., *J. Clin. Invest. 97*:1557-1560 (1996), and Strojek, R.M. and Wagner, T.E., *Genetic Engineering: Principles and Methods 10*:221-246 (1988), which supposedly illustrate the technical difficulties associated with producing transgenic animals that exhibit a particular phenotype.

The technical considerations cited by the Examiner do not suggest that producing transgenic animals with particular phenotypes would have required undue experimentation. In fact, Wall and Mullins both describe examples of the successful production of transgenic animals with specific desired phenotypes. (*See* the January 22, 2003 response, pages 28-29.) As discussed below, the numerous examples in the scientific literature of the successful production of transgenic animals that display desired phenotypes indicates that it would not have required undue experimentation to make and use the transgenic animals of the invention.

It was also asserted that:

> the specification fails to provide any relevant teachings or sufficient guidance with regards to the production of any transgenic non-human animals comprising a transgenic sequence encoding SEQ ID NO: 1 or a sequence with 90% homology thereto, which over-expresses the transgenic sequence such that a phenotype occurs.

(Paper No. 16, page 10.) Applicants respectfully disagree. The specification describes exemplary methods for obtaining transgenic animals including, *e.g.*, injecting a DNA construct into a fertilized egg which is allowed to develop into an adult animal, and generating transgenic animals with embryonic stem cell technology. (*See* specification at page 20, lines 3-17.) The specification also cites and incorporates by reference several references which describe additional methods of preparing transgenic animals. (*See* specification at page 20, lines 18-25.)

There are numerous examples in the scientific literature of the production of transgenic animals exhibiting specific desired phenotypes. Applicants have previously submitted several such examples. (*See* the August 8, 2002 response at pages 31-32, and Exhibits B-E attached thereto.) With respect to these examples, the Examiner stated that

"the exhibits do not provide sufficient guidance or factual evidence for producing the claimed transgenic non-human animal. In addition, the exhibits do not use the same method and materials as contemplated by the specification." (Paper No. 16, page 15.)

The fact that the exhibits do not demonstrate the production of the "claimed transgenic non-human animal" does not support a finding of non-enablement. "The mere fact that something has not previously been done clearly is not, in itself, a sufficient basis for rejecting all applications purporting to disclose how to do it." *Gould v. Quigg*, 822 F.2d 1074, 1078, 3 USPQ2d 1302, 1304 (Fed. Cir. 1987) (quoting *In re Chilowsky*, 229 F.2d 457, 461, 108 USPQ 321, 325 (CCPA 1956)).

In addition, it is incorrect that the methods exemplified in the exhibits are not "contemplated by the specification." The specification makes clear that any method known to those skilled in the art can be used for the production of the transgenic animals of the invention. (*See, e.g.*, specification at page 20, lines 18-19, citing and incorporating by reference U.S. Patent No. 5,602,299, describing numerous methods known in the art; *see also* the August 8, 2002 response at page 21.) Thus, the methods used in exhibits B-E, which were known and available as of the effective filing date of the application, were contemplated by the specification.

The fact that there are numerous examples in the art of successfully produced transgenic animals expressing specific desired phenotypes indicates that the production of the transgenic animals of the invention would not have required undue experimentation.

The Examiner referred to the following sentence from de la Monte and Wands, *J. Neuropathol. Exp. Neurol. 60*:195-207 (2001):

> Although initial studies suggested that AD7c-NTP over-expression might contribute to AD neurodegeneration by

> promoting cell death, we were unable to investigate this issue using standard stably transfected cells because of progressive depletion of the cells in culture, which probably died due to apoptosis induced by AD7c-NTP expression.

(de la Monte and Wands, sentence bridging pages 203-204, internal citation omitted, referred to in Paper No. 16, page 16.) Based on this sentence, the Examiner asserted that "the specification does not provide sufficient guidance for one skilled in the art to over-express AD7c-NTP in cells of an animal and avoid depletion of cells resulting in death of the animal." (Paper No. 16, page 16.) Applicants do not agree that over-expression of a DNA molecule of SEQ ID NO:1 or a DNA molecule which is at least 90% homologous thereto in one or more cells of the claimed transgenic animals would necessarily result in death of the animals. Nonetheless, the eventual death of the transgenic animals due to over-expression of SEQ ID NO:1 or a DNA molecule that is at least 90% homologous thereto does not indicate that producing the transgenic animals would have required undue experimentation or that the animals could not have been used in drug screening applications prior to the time of death.

Finally, the Examiner cited four references that supposedly show "the unpredictability of making an animal model using amyloid Beta protein, which is also over-expressed in the brain of patients with AD." (Paper No. 16, page 16, citing Mucke *et al.*, *Brain Res. 666*:151-167 (1994), Sandhu, *Age 17*:7-11 (1994), Malherbe *et al.*, *Neurobiol. Aging 17*:205-214 (1996), and Loring *et al.*, *Neurobiol. Aging 17*:173-182 (1996).) The cited references, however, do not indicate that the production of transgenic animals expressing an Alzheimer's disease-related transgene (Aβ) would have required undue experimentation. In fact, all of these references demonstrate the successful production of transgenic animals.

In addition, there are numerous other examples from the scientific literature showing the successful production of transgenic animals expressing amyloid beta genes or variants thereof, *wherein the transgenic animals displayed neurological phenotypes indicative of Alzheimer's disease.* Exemplary references include Quon *et al.*, *Nature 352*:239-241 (1991) (copy included herewith as Exhibit A); Wirak *et al.*, *Science 253*:323-325 (1991) (copy included herewith as Exhibit B); Kammesheidt *et al.*, *Proc. Natl. Acad. Sci. USA 89*:10857-10861 (1992) (copy included herewith as Exhibit C); Games *et al.*, *Nature 373*:523-527 (1995) (copy included herewith as Exhibit D); and Johnson-Wood *et al.*, *Proc. Natl. Acad. Sci. USA 94*:1550-1555 (1997) (copy included herewith as Exhibit E). These references provide further evidence that the transgenic animals of the present invention could have been made and used without undue experimentation.

### *3. Summary*

A person of ordinary skill in the art, in view of the specification, would have been able to make and use the transgenic animals of the invention using routine methods that were well known in the art. No evidence or sound scientific arguments have been presented to explain why, despite the fact that numerous examples of the successful production of transgenic animals existed in the scientific literature, the production of the transgenic animals of the present invention would have required undue experimentation. Applicants therefore respectfully request that the enablement rejection of claims 7-9, 14-16 and 35-40 be reconsidered and withdrawn.

## *Conclusion*

All of the stated grounds of objection and rejection have been properly traversed, accommodated, or rendered moot. Applicants therefore respectfully request that the Examiner reconsider all presently outstanding objections and rejections and that they be withdrawn. Applicants believe that a full and complete reply has been made to the outstanding Office Action. If the Examiner believes, for any reason, that personal communication will expedite prosecution of this application, the Examiner is invited to telephone the undersigned at the number provided.

Prompt and favorable consideration of this Reply is respectfully requested.

Respectfully submitted,

STERNE, KESSLER, GOLDSTEIN & FOX P.L.L.C.

Frank R. Cottingham

Frank R. Cottingham
Attorney for Applicants
Registration No. 50,437

Date: July 7, 2003

1100 New York Avenue, N.W.
Washington, D.C. 20005-3934
(202) 371-2600

# EXHIBIT A

# Formation of β-amyloid protein deposits in brains of transgenic mice

D. Quon, Y. Wang, R. Catalano, J. Marian Scardina, K. Murakami* & B. Cordell†

California Biotechnology Inc., 2450 Bayshore Parkway, Mountain View, California 94043, USA
* Present address: Research Institute, Daiichi Pharmaceutical Co., 16-13, Kita-kasi 1-Chome Edogawa-ku, Tokyo 134, Japan
† To whom correspondence should be addressed

**DEPOSITS of β-amyloid are one of the main pathological characteristics of Alzheimer's disease. The β-amyloid peptide constituent (relative molecular mass 4,200) of the deposits is derived from the β-amyloid precursor protein (β-APP) which is expressed in several different isoforms[1–6]. The two most prevalent β-APP isoforms are distinguished by either the presence (β-APP751) or absence (β-APP695) of a Kunitz serine protease inhibitor domain. Changes in the abundance of different β-APP messenger RNAs in brains of Alzheimer's disease victims have been widely reported[7–12]. Although these results have been controversial, most evidence favours an increase in the mRNAs encoding protease inhibitor-containing isoforms of β-APP and it is proposed that this change contributes to β-amyloid formation[9–12]. We have now produced an imbalance in the normal neuronal ratio of β-APP isoforms by preparing transgenic mice expressing additional β-APP751 under the control of a neural-specific promoter. The cortical and hippocampal brain regions of the transgenic mice display extracellular β-amyloid immunoreactive deposits varying in size (<5–50 μm) and abundance. These results suggest that one mechanism of β-amyloid formation may involve a disruption of the normal ratio of neuronal β-APP isoform expression and support a direct relationship between increased expression of Kunitz inhibitor-bearing β-APP isoforms and β-amyloid deposition.**

A chimaeric gene was constructed between the human β-APP751 complementary DNA and the rat neural-specific enolase (NSE) promoter, termed NSE: β-APP751. The rat NSE promoter directs the neural-specific expression of β-galactosidase in transgenic mice[13] and we have confirmed this using a NSE promoter fragment slightly truncated at the 5′ terminus (our unpublished results). The promoter fragment containing the 5′ untranslated region of NSE and a roughly 1.2-kilobase (kb) intron in this domain was fused to the β-APP751 cDNA such that the initiator methionine of NSE was replaced with the initiator methionine of β-APP751. Nine of 44 mice that developed from embryos injected with NSE:β-APP751 DNA carried the transgene. Three pedigrees were selected for extensive characterization: founders 10 (F10), 11 (F11) and 24 (F24). Homo- and hemizygotic states and transgene copy numbers were determined by comparison to the endogenous single copy β-APP mouse gene using Southern blot hybridization with a probe common to both mouse β-APP and human β-APP751 (Table 1).

RNA expression of the inherited transgenes in the three pedigrees was investigated. Total brain RNA was isolated both from positive and from wild-type control animals, reverse transcribed, and a specific DNA subfragment amplified by polymerase chain reaction (PCR). Primers for PCR were designed such that only transcripts derived from the transgene would be amplified, that is, one primer hybridizes to the NSE 5′ untranslated region and the other to the 5′ coding domain of β-APP. The NSE PCR primer corresponds to a site located upstream of the intron so that amplification of contaminating genomic DNA or unprocessed transcripts could be detected. A predicted 373-base pair (bp) fragment is amplified from reverse-transcribed RNA prepared from each transgenic animal but not from wild-type mice (Fig. 1*a*). As a control, half of the reverse-transcribed RNA was amplified with a primer for the native

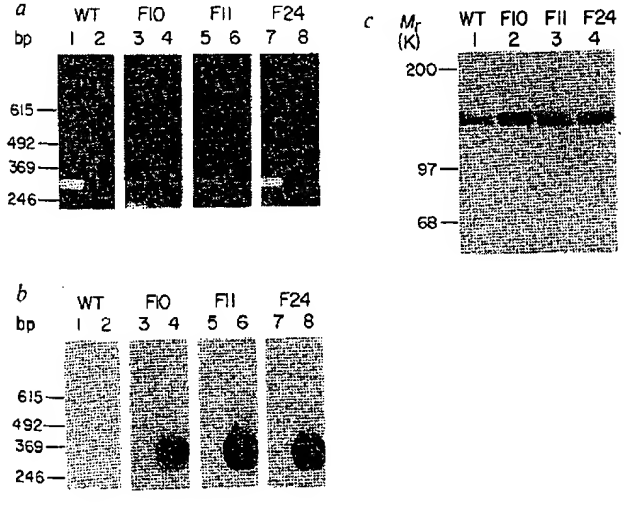


FIG. 1 NSE: β-APP751 expression in brain. *a*, Agarose gel electrophoresis of reverse transcribed PCR products visualized with ethidium bromide staining. Even numbered lanes, reverse transcribed PCR products from wild-type (WT), NSE: β-APP751 founder 10 (F10), founder 11 (F11) and founder 24 (F24) RNA primed with primers specific for NSE: β-APP751 RNA. Odd numbered lanes, reverse-transcribed PCR products from RNA primed with primers specific for endogenous β-APP RNA. *b*, Southern blot of above reverse-transcribed PCR products using $^{32}$P-labelled oligonucleotide probe specific for the NSE: β-APP751 chimaeric gene. Lanes are the same as in *a*. *c*, Western blot analysis of β-APP in brain. Lane 1, WT; 2, F10; 3, F11; 4, F24 total brain protein immunoblotted with β-APP antiserum.

METHODS. An ~8-kb rat genomic fragment containing the NSE gene was isolated on the basis of the published sequence[22] and the 2.3-kb fragment used for the chimaeric gene isolated by PCR. PCR primers were designed to generate *Bgl*II and *Nco*I sites at the 5′ and 3′ terminus of the fragment, respectively. A *Nru*I(position 123)–*Xmn*I(position 2,665) fragment was isolated from β-APP751 cDNA[4], and was ligated with the 2.3-kb NSE fragment harboured in a derivative of pcDV1 plasmid containing the simian virus 40 (SV40) late region polyadenylation signal[23]. A linear fragment of NSE: β-APP751 was prepared by cleavage with *Sal*I and *Nde*I and was injected into fertilized embryos of the JU strain of mouse[24]. The JU strain, developed by Eric Bradford at the University of California Davis, was chosen for its large litter size. For genotype and copy number determinations, 40 μg of tail DNA was digested with *Bgl*II and electrophoresed on 0.8% agarose gels. Southern blots were prepared[25] and hybridized with an oligonucleotide probe (5′-ATGGATGTGTACTGTTTCTTCTTCA-3′) radiolabelled with $^{32}$P by T4 kinase. Blots were hybridized at 60 °C in 6 × SET (1 × SET = 0.15 M NaCl, 30 mM Tris-HCl pH 8.0, 2 mM EDTA) with 5 × Denhardt's solution and washed at 60 °C for 40 min in 6 × SSC (1 × SSC = 0.15 M NaCl, 0.015 M Na-citrate). For transcriptional analyses, 2 μg of total brain RNA was reverse transcribed with oligo(dT)$_{12-18}$, after which the reaction was divided into two equal aliquots. PCR[26] was done on one aliquot using NSE (5′-CACCGCCACCGGCTG-AGTCTGCAGTCCTCG-3′) and β-APP (5′-TCTTGCACTGCTTGCGGCCCCGCTT-GCACC-3′) primers and on the second aliquot with the same β-APP primer and a primer to the secretory signal sequence of β-APP (5′-TTGGCACTGCT-CCTGCTGGCCGCCTGGACG-3′) in place of the NSE primer. DNA products were electrophoresed on 2% agarose gels, visualized by staining with ethidium bromide, then Southern blotted[25] and hybridized with a $^{32}$P-labelled oligonucleotide probe to the NSE: β-APP751 fusion sequence (5′-AGATCCCAGC-CACCGATGCTGCCCGGTTTG-3′). Blots were hybridized at 65 °C in 6 × SET and washed at 65 °C for 40 min in 4 × SSC. Protein homogenates were made from total brain[14] and 50 μg of each sample was electrophoresed on 7.5% SDS–polyacrylamide gels[27]. A western blot[28] was developed using a 1:500 dilution of antiserum and $^{125}$I-labelled protein A. The antiserum was raised against full-length human β-APP695 expressed by a recombinant vaccinia virus[16]. Identically prepared gels stained with Coomassie blue dye confirmed that equivalent amounts of protein were loaded for each sample.

β-APP secretory signal sequence and the same 5′ coding domain β-APP primer to produce a 307-bp DNA fragment representing amplification from endogenous β-APP RNA (Fig. 1*a*). When all the PCR reaction products are hybridized with a probe bridging the junction between NSE and β-APP751 sequences, only the products derived from the transgenic brains hybridize, documenting the authenticity of the 373-bp PCR product (Fig. 1*b*).

Western blots were made to evaluate changes in protein expression in the brains of the transgenic animals. Equal amounts of total protein from whole brain homogenates were electrophoresed on polyacrylamide gels, transferred to a membrane then reacted with polyclonal serum raised against full-length β-APP. A band (or set of unresolved bands) of relative molecular mass of about 130,000 (130K), corresponding to the reported average size of mammalian brain β-APP isoforms[14–16], is observed in the control, as well as in each transgenic protein homogenate (Fig. 1*c*). This signal is increased in the NSE:β-APP751 samples relative to the wild-type sample suggesting globally elevated β-APP751 expression in the transgenic brains. To obtain a more refined examination of NSE:β-APP751 expression and its effects, we used immunocytochemistry.

A panel of monoclonal antibodies was prepared using a synthetic peptide corresponding to residues 1–28 of the β-amyloid protein as the immunogen. The specificity of the monoclonals was established by immunoperoxidase staining of brain sections from Alzheimer's disease victims (Fig. 2 *a*, *b*). Sections were prepared from brains of NSE:β-APP751 transgenic mice, as well as from wild-type mice and both were stained in parallel with one monoclonal, 4.1 (Table 1). Reproducibly greater immunoperoxidase reactivity is observed in neurons and as fine puncta throughout the neuropil of the transgenic brains compared with the immunoreactivity visualized in brains from wild-type mice. A pronounced staining of neuritic processes is also noticeable (Fig. 2*d*). This enhancement of arbor-forming neuronal processes is most evident in the stratum flanking the pyramidal cell layer of the CA-1 and CA-3 regions of transgenic hippocampi. Both neuronal and process staining are fully competed by earlier incubation of the antibody with the synthetic β-amyloid peptide. Neuritic staining in the transgenic brains is also detected using antibodies raised against full-length β-APP (Fig. 2*c*), indicating full-length β-APP is present in the neuritic

TABLE 1 Summary of mice used for immunohistology

| Line | Animal | Sex | Age* | Genotype | Copy number† | Deposits‡ |
|---|---|---|---|---|---|---|
| NSE:β-APP751 | | | | | | |
| 10 | 0 | F | 12 | Aa | 1 | +++ |
| | 31§ | F | 7 | Aa | | ++ |
| | 168 | F | 5 | Aa | | +++ |
| | 334 | M | 2 | AA | | + |
| 11 | 0 | M | 15 | Aa | 4 | +++ |
| | 51 | M | 12 | Aa | | + |
| | 236 | M | 4 | AA | | +++ |
| | 287 | F | 3 | AA | | + |
| 24 | 77 | M | 8 | Aa | 8 | + |
| | 201 | F | 5 | AA | | + |
| Wild type | | | | | | |
| | 1 | F | 4 | NA | NA | — |
| | 2 | F | 4 | | | — |
| | 3 | M | 5 | | | — |
| | 4 | M | 3 | | | — |
| | 5 | M | 9 | | | — |
| | 6 | F | 12 | | | — |
| | 7 | M | 14 | | | — |

M and F indicate male and female mice, respectively; AA and Aa represent homozygotic and hemizygotic animals, respectively; NA, not applicable.
* Months.
† Haploid.
‡ >5 μm in size, (–) none, (+/++/+++) relative abundance of deposits, that is, + indicates <5; ++ indicates 5–10; +++ indicates >10 deposits per section as an average of multiple sections stained.
§ NSE: β-APP751 F10, number 31 died of unknown cause.

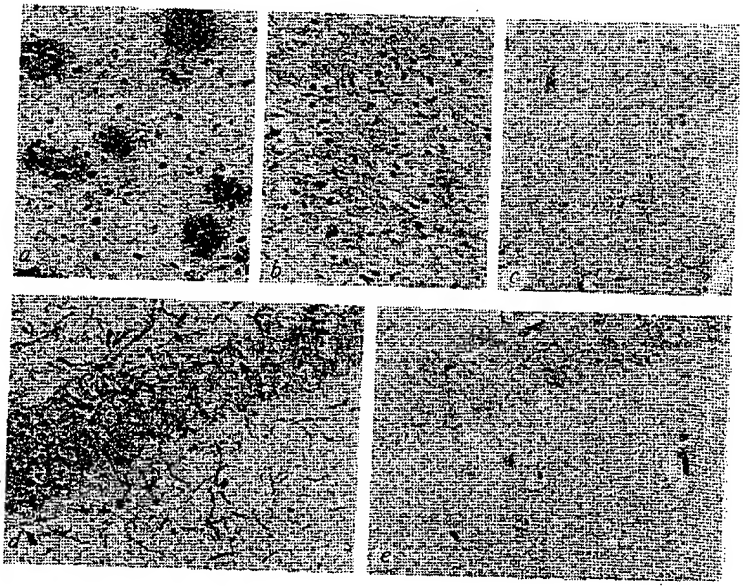

FIG. 2 Immunoperoxidase staining of human and mouse brain. Human Alzheimer's disease tissue section from caudal hippocampus stained with 4.1 antibody without (*a*) and an adjacent section (*b*) with preincubation with the β-amyloid synthetic peptide immunogen (×250). Hippocampal CA-1 field of NSE: β-APP751 F10 (number 334) stained with antibodies to full-length β-APP (*c*); pyramidal cell layer of CA-1 region from NSE: β-APP751 F10 (number 334) stained with 4.1 antibody (*d*); same region from wild-type mouse (number 3) identically stained with 4.1 antibody (*e*) (×500).

METHODS. A synthetic peptide corresponding to residues 1–28 of the β-amyloid protein[1,2] was prepared and self-aggregated by freezing and thawing. The peptide aggregate was mixed with methylated bovine serum albumin and adjuvant for immunizing and boosting mice. Hybridomas from the sensitized spleen cells were generated[29]. Clones secreting anti-peptide antibodies were expanded and subcloned by limiting dilution. The epitope recognized by each monoclonal was mapped to the N-terminal 10 residues of the β-amyloid protein. For analysis of mouse brains, brains were removed and fixed with 4% paraformaldehyde, embedded in paraffin and 6 μm coronal midbrain sections made. Sections were deparaffinized, rehydrated, treated for 30 min with 0.3% $H_2O_2$, then with 80% formic acid for ~2 min. Sections were next incubated at 37°C for 30 min with a 1/20 dilution of conditioned medium from the hybridoma secreting the 4.1 antibody. An anti-mouse avidin-biotinylated horseradish peroxidase (ABC) kit was used according to supplier's recommendations (Vector, Burlingame, California) and the horseradish peroxidase visualized with 3,3′-diaminobenzidine. Staining for full-length β-APP used the antiserum used for western blotting in *c* at a 1:500 dilution and an anti-rabbit ABC kit. Formic acid treatment was omitted for β-APP staining. Sections were counterstained with haematoxylin and eosin. Human brain sections were from individuals clinically diagnosed with Alzheimer's disease. The human sections were prepared and stained identically as mouse tissue sections except they were treated with 98% formic acid for 10 min. For competition experiments, the antibody diluent was preincubated at 4 °C for 12 h then 37 °C for 30 min with 250 μg $ml^{-1}$ 1–28 β-amyloid synthetic peptide before application. Congo red, thioflavin S and silver staining were done using published procedures[18–21,30].

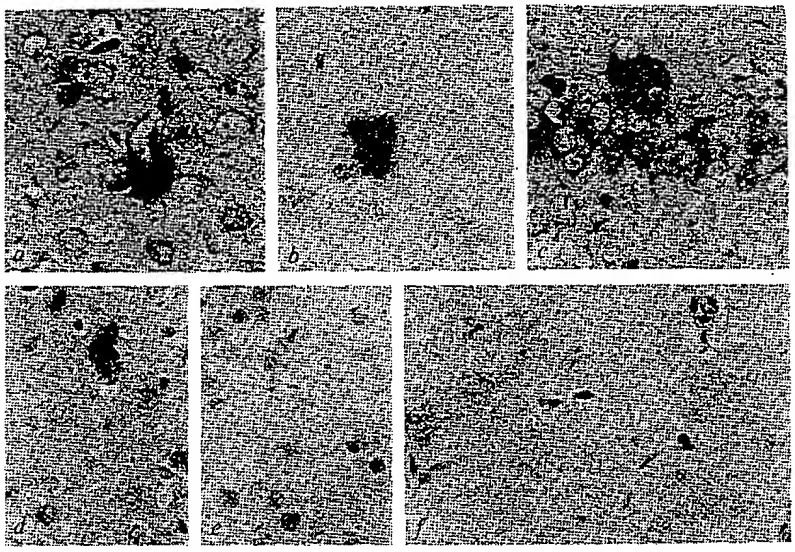

FIG. 3 Immunoreactive deposits in NSE:β-APP751 brains. *a*, Compact deposit in frontalparietal cortex of F11 (number 0); *b*, compact deposit in thalamus of F11 (number 236); *c*, compact deposit in hippocampal CA-2 field of F11 (number 0); *d*, cluster of deposits in frontalparietal cortex of F10 (number 168); *e*, adjacent section as in *d* but antibody preincubated with β-amyloid synthetic peptide before staining (arrowheads demark same capillaries in field of *d* and *e*); *f*, amorphous deposits in the hippocampal stratum moleculare of F11 (number 236) (×500). Immunocytochemistry and competition were performed as described in the legend to Fig. 2.

processes, although the possibility that the neurites also contain β-amyloid protein cannot be excluded.

Extracellular immunoreactive deposits are also consistently seen in the brain sections from each of the three transgenic lines stained with the 4.1 monoclonal which are not seen in sections from wild-type animals identically stained. The immunoreactive deposits vary in size, shape and frequency. Examples of compact deposits 10–50 μm in diameter are shown in Fig. 3*a–d*. These immunoreactive deposits tend to occur in clusters and are most frequently observed in the cortex and hippocampus although occasionally they have been found in the thalamus and striatum. A second type of immunoreactive extracellular deposit is reproducibly seen in transgenic brain sections which is lacking in control brain sections. This type of deposit is diffuse, amorphous and granular (Fig. 3*f*). Detection of extracellular deposits in the tissue sections from the transgenic animals required treatment with formic acid. Immunoreactivity of these structures also could be competed by the β-amyloid peptide (Fig. 3*e*). In a preliminary survey, antibodies to full-length β-APP stained extracellular deposits of similar morphology as those stained by the 4.1 monoclonal. Also, in general, the deposits are stained by silver salts, infrequently by thioflavin S, but not by Congo red, corroborating a preamyloid-like composition (data not shown). Owing to the small group of animals analysed, it is difficult to make a correlation between the frequency of deposit appearance with age, genotype or sex (Table 1).

Although there may exist several different mechanisms promoting β-amyloid formation[17], the observed increased level of Kunitz inhibitor-containing β-APP isoform RNA in neurons of Alzheimer's disease brains suggests that Kunitz inhibitor β-APP isoform overexpression may be one mechanism[9–12]. The three NSE:β-APP751 transgenic lines which have moderately increased neuronal expression of β-APP751 and form extracellular β-amyloid immunoreactive deposits (as well as our preliminary data on NSE:β-APP695 transgenic lines which do not) support this hypothesis. The two types of extracellular deposits, diffuse and compact, seen in the transgenic mice resemble several β-amyloid structures typically seen in the brains of Alzheimer's disease victims, specifically preamyloid and preamyloid plaques[18–21]. It will be of interest to determine whether the quality and/or quantity of deposits change in an age-dependent manner and if the mice display other pathological features characteristic of Alzheimer's disease. □

Received 31 January; accepted 25 June 1991.

1. Glenner, G. G. & Wong, C. W. *Biochem. biophys. Res. Commun.* **120**, 885–890 (1984).
2. Masters, C. L. *et al. Proc. natn. Acad. Sci. U.S.A.* **82**, 4245–4249 (1985).
3. Kang, J. *et al. Nature* **325**, 733–736 (1987).
4. Ponte, P. *et al. Nature* **331**, 525–528 (1988).
5. Tanzi, R. E. *et al. Nature* **331**, 528–530 (1988).
6. Kitaguchi, N., Takahashi, Y., Tokushima, Y., Shiojiri, S. & Ito, H. *Nature* **331**, 530–532 (1988).
7. Palmert, M. R. *et al. Science* **241**, 1080–1084 (1988).
8. Neve, R. L., Finch, E. A. & Dawes, L. R. *Neuron* **1**, 669–677 (1988).
9. Johnson, S. A. *et al. Expl Neurol.* **102**, 264–268 (1988).
10. Tanaka, S. *et al. Biochem. biophys. Res. Commun.* **157**, 472–479 (1988).
11. Johnson, S. A., McNeill, T., Cordell, B. & Finch, C. E. *Science* **248**, 854–857 (1990).
12. Neve, R. L., Rogers, J. & Higgens, G. A. *Neuron* **5**, 329–338 (1990).
13. Forss-Petter, S. *et al. Neuron* **5**, 187–197 (1990).
14. Shivers, B. D. *et al. EMBO J.* **7**, 1365–1370 (1988).
15. Takio, K., Hasegawa, M., Titani, K. & Ihara, Y. *Biochem. biophys. Res. Commun.* **160**, 1296–1301 (1989).
16. Murphy, G. M. *et al. Prog. Neuro-psychopharmac.* **14**, 309–317 (1990).
17. Goate, A. *et al. Nature* **349**, 704–706 (1991).
18. Yamaguchi, H., Hirai, S., Morimatsu, M., Shoji, M. & Ihara, Y. *Acta neuropath.* **76**, 541–549 (1988).
19. Tagliavini, F., Giaccone, G., Frangione, B. & Bugiani, O. *Neurosci. Lett.* **103**, 191–196 (1988).
20. Ikeda, S., Allsop, D. & Glenner, G. G. *Lab. Invest.* **60**, 113–122 (1989).
21. Bugiani, O., Giaconne, G., Frangione, B., Ghetti, B. & Tagliavini, F. *Neurosci. Lett.* **103**, 263–268 (1989).
22. Sakimura, K., Kushiya, E., Takahashi, Y. & Suzuki, Y. *Gene* **60**, 103–113 (1987).
23. Okeyama, H. & Berg, P. *Mol. cell. Biol.* **3**, 280–289 (1983).
24. Eklund, J. & Bradford, G. E. *Anim. Prod.* **22**, 127–130 (1976).
25. Southern, E. M. *J. molec. Biol.* **98**, 503–517 (1975).
26. Saiki, R. K. *et al. Science* **239**, 487–491 (1988).
27. Laemmli, U. K. *Nature* **227**, 680–685 (1970).
28. Tobin, H., Staehelin, T. & Gordon, J. *Proc. natn. Acad. Sci. U.S.A.* **76**, 4350–4354 (1979).
29. Taggart, R. T. & Samloff, I. M. *Science* **219**, 1228–1230 (1983).
30. Allsop, D. *et al. Neuropath. appl. Neurobiol.* **15**, 531–542 (1989).

ACKNOWLEDGEMENTS. We thank G. Anderson, S. Donahue and A. Moyer for performing transgenic embryology, A. Lam, U. Masharani, L. Carstensen and P. Hummel for their technical assistance and contributions in the development and care of transgenic animals. T. Finch for providing human brain sections, G. Murphy for viewing stained tissue sections, and E. Stoelting for artwork. This work was supported by Daiichi Pharmaceutical Co. of Tokyo, Japan.

# Spontaneous calcium release from inositol trisphosphate-sensitive calcium stores

**Ludwig Missiaen*, Colin W. Taylor† & Michael J. Berridge***

* AFRC Laboratory of Molecular Signalling, Department of Zoology, University of Cambridge, Downing Street, Cambridge CB2 3EJ, UK
† Department of Pharmacology, University of Cambridge, Tennis Court Road, Cambridge CB2 1QJ, UK

**Inositol 1,4,5-trisphosphate ($InsP_3$) functions as a second messenger to mobilize $Ca^{2+}$ from intracellular reservoirs[1]. The release mechanism displays all-or-none characteristics[2,3], that may account for other observations that the $InsP_3$-induced mobilization of $Ca^{2+}$ is quantal[4–6]. Quantal release may depend on the sensitivity of the $InsP_3$ receptor being regulated by the $Ca^{2+}$ concentration in the lumen of the endoplasmic reticulum[7]. We report here that**



# nature

**11 July 1991**

**Vol. 352 Issue no. 6332**


◀ The second brightest globular cluster in the sky, NGC104 or 47 Tucanae, is now shown to host not one but 11 millisecond pulsars (pages 219 and 195), bringing the present count to 23. 'Wind' from such pulsars could explain the relative lack of gas in globular clusters, page 221. (Photo: ESO.)

## THIS WEEK . . . THIS WEEK . . . THIS WEEK . . .

### thirtysomething

Alkali-metal-doped compounds of $C_{60}$ fullerenes are proving fertile ground for the search for high-temperature superconductors. Potassium and rubidium doping are known to produce superconducting phases, but now two labs report superconductivity at and above 30 K using caesium (page 223) and caesium/rubidium dopants (see page 222).

### Seventh gear

Development of the R7 photoreceptor in the *Drosophila* eye involves an interaction requiring expression of the cell surface receptor encoded by *sevenless* gene in R7 cells and *bride of sevenless* in R8 cells. On page 207, Krämer *et al.* demonstrate that 'boss', a protein on the surface of R8, interacts directly with sev on R7, and that the boss protein is actually taken up by the R7 cells by receptor-mediator endocytosis. News and Views page 193.

### *Rb* function

The function of the product of the retinoblastoma gene in normal cells is a negative regulator of cellular proliferation. Wild-type retinoblastoma protein forms a complex with a cellular transcription factor; on page 249 this complex is shown also to contain cyclin A and a naturally occurring mutant of *Rb* is reported to be unable to form this complex. In a separate experiment (page 251), the cloning of genes encoding two human cellular proteins that bind to the *Rb* product in competition with DNA tumour virus transforming proteins is reported. News and Views page 189.

### Fish course

The earliest-known land vertebrate, *Acanthostega*, had fish-like internal gills, suggesting that it retained far more of an aquatic lifestyle than has been realized. Page 234.

### Sulphur count

Radioactive sulphur-35, produced by cosmic-ray bombardment in the upper atmosphere, provides a marker with potential as a worldwide measure of $SO_2$ oxidation and sulphate removal rates. Aerosol sulphate is thought to play a role in tropospheric heat balance, and is therefore relevant to the issue of global warming. See page 226.

### Fatherly figures

Strict maternal inheritance of mitochondrial DNA is the norm in animals, but using interspecific mouse backcrosses and PCR techniques, Gyllensten *et al.* are able to show that sperm contribute approximately 1/1,000 of the total mitochondrial DNA to the zygote. Page 255.

### Alzheimer model

Transgenic mice into which the gene encoding a putative pathological isoform of the β-amyloid protein has been introduced develop lesions resembling those seen in human Alzheimer's disease. Page 239.

### Natural selection

Synthesis gas, a mixture of hydrogen and carbon monoxide, is the starting material for the industrial preparation of many organic compounds. A new strategy for converting natural gas to synthesis gas offers the prospect of a synthesis route with some engineering advantages. Page 225.

### Speech recognition

Cochlear implants can give profoundly deaf subjects some hearing ability by converting sound into direct electrical stimulation of the auditory nerve. A new processing strategy gives a significant improvement in the ability of subjects with cochlear implants to recognize speech. Page 236.

### Guide to Authors

Inside back cover.



*Nature*® (ISSN 0028-0836) is published weekly on Thursday, except the last week in December, by Macmillan Magazines Ltd (4 Little Essex Street, London WC2R 3LF). Annual subscription for USA and Canada US$350 (institutional/corporate). US$135 (individual making personal payment). US and Canadian orders to: *Nature*, Subscription Dept, PO Box 1733, Riverton, NJ 08077-7333, USA. Other orders to *Nature*, Brunel Road, Basingstoke, Hants RG21 2XS, UK. Second class postage paid at New York, NY 10012, and additional mailing offices. Authorization to photocopy material for internal or personal use, or internal or personal use of specific clients, is granted by *Nature* to libraries and others registered with the Copyright Clearance Centre (CCC) Transactional Reporting Service, provided the base fee of $1.00 a copy plus $0.10 a page is paid direct to CCC, 27 Congress Street, Salem, MA 01970, USA. Identification code for *Nature*: 0028-0836/91 $1.00 + $0.10. US Postmaster send address changes to: Nature, 65 Bleecker Street, New York, NY 10012. Published in Japan by Nature Japan K.K., Shin-Mitsuke Bldg. 36 Ichigaya Tamachi, Shinjuku-ku, Tokyo 162, Japan 

# EXHIBIT B

tisense 1220) were used for the initial amplification, and K3 5′-TAGAACGATTCGCAGTTAAT (*gag* sense 913) and K7 5′-CCTGGATGTTCTGCACTATA (*gag* antisense 1207) were used for the nested amplification. The transferred product was probed with a fragment of pHXB2D (nucleotides 631 to 1258) labeled with deoxyadenosine triphosphate, deoxycytidine triphosphate, and deoxyguanidine triphosphate by the random priming method to a specific activity of $1.14 \times 10^8$ cpm per milligram of DNA.

32. Supported by PHS program projects NS-27405, NS-11037, and CA-45690, and a grant from the W. W. Smith Charitable Trust (to F.G.-S.). S.B. is also supported by a grant from the National Multiple Sclerosis Society, and S.L.S. is a Mallinckrodt Scholar. We thank B. Godfrey for raising antibody 8586, D. Kolson, R. Collman, and T. Brown for fluorescence microscopy, L. Lynch for technical assistance, C. Griot for providing MAb 16G1, P. McGonigle for help with the Scatchard plot, and J. Hoxie, S. Miller, N. Nathanson, A. K. Asbury, and members of the Nathanson/Gonzalez laboratories for helpful comments and encouragement. We also thank J. Burns (University of Utah).

12 December 1990; accepted 24 May 1991



# Deposits of Amyloid β Protein in the Central Nervous System of Transgenic Mice

D. O. WIRAK,* R. BAYNEY, T. V. RAMABHADRAN,† R. P. FRACASSO, J. T. HART, P. E. HAUER, P. HSIAU, S. K. PEKAR, G. A. SCANGOS, B. D. TRAPP, A. J. UNTERBECK‡

**Alzheimer's disease is characterized by widespread deposition of amyloid in the central nervous system. The 4-kilodalton amyloid β protein is derived from a larger amyloid precursor protein and forms amyloid deposits in the brain by an unknown pathological mechanism. Except for aged nonhuman primates, there is no animal model for Alzheimer's disease. Transgenic mice expressing amyloid β protein in the brain could provide such a model. To investigate this possibility, the 4-kilodalton human amyloid β protein was expressed under the control of the promoter of the human amyloid precursor protein in two lines of transgenic mice. Amyloid β protein accumulated in the dendrites of some but not all hippocampal neurons in 1-year-old transgenic mice. Aggregates of the amyloid β protein formed amyloid-like fibrils that are similar in appearance to those in the brains of patients with Alzheimer's disease.**

ACCUMULATION OF AMYLOID β PROTEIN is a characteristic and diagnostic feature of brains from individuals with Alzheimer's disease (AD) and Down syndrome (DS) (*1*). The 4-kD amyloid β protein is a truncated form of a larger amyloid precusor protein (APP), which has features typical of a cell surface integral membrane glycoprotein (*2*). At least five different APP isoforms containing 563, 695, 714, 751, and 770 amino acids (*3*) can be generated by alternative splicing of primary transcripts of a single gene on chromosome 21 (*3*). The 40– to 42–amino acid β protein segment comprises half of the transmembrane domain and the first 28 amino acids of the extracellular domain of APP (*2*), and is encoded within two exons (*4*).

The mechanism by which the amyloid β protein is derived from its precursor is not known. APP is processed in vitro by a proteolytic cleavage within the amyloid β protein region (*5*). Generation of the amyloid β protein, therefore, involves an alternative processing pathway, possibly as a result of post-translational modifications such as phosphorylation (*6*).

Although the deposition of amyloid appears to be an early event in the progression of AD (*7*), its role in neurodegenerative processes remains unknown. Amyloid β protein can be neurotrophic for undifferentiated hippocampal neurons in culture and, at high concentrations, neurotoxic to differentiated neurons (*8*). Mutant forms of APP have been implicated in hereditary cerebral hemorrhage with amyloidosis of Dutch origin (*9*) and in at least two families with familial forms of AD (*10*). In addition, overexpression of one or more forms of APP may be responsible for the AD-like pathologies of individuals with DS (*11*). These findings suggest that accumulation of amyloid β protein may be a critical step in the neurodegenerative processes of AD.

The lack of experimental animal models for AD has limited the elucidation of the mechanism of amyloid formation and its role in the pathogenesis of AD. Nonhuman primates provide the only in vivo model for investigating amyloid formation in the central nervous system (CNS) (*12*). The high cost and limited availability of aged primates, however, restricts their use as practical model systems. Transgenic rodent models may provide a useful alternative. The expression of native or mutant forms of APP in transgenic mice may help to identify aberrant APP processing pathways that lead to the accumulation of amyloid β protein and clarify the role of amyloid β protein in neuronal degeneration. We therefore initiated a series of experiments to express various forms of APP in the brain of transgenic mice.

We have introduced into mice a construct that encodes the 42–amino acid amyloid β protein, regulated by a 4.5-kb fragment from the 5′ region of the human APP gene (Fig. 1). This APP regulatory region directs neuron-specific expression of the reporter gene *lac Z* from *Escherichia coli* in the CNS of transgenic mice in a pattern that is similar to the pattern of endogenous mouse and human APP mRNA expression (*13*).

Two lines of transgenic mice, AE101 and AE301, expressed human amyloid β protein mRNA in the brain (Fig. 2) and transmitted the transgene in a Mendelian fashion. Steady-state amounts of the transgene mRNA were lower than steady-state amounts of the endogenous mouse APP mRNA. In both transgenic lines, however, human amyloid β protein was synthesized and accumulated in the CNS of 1-year-old mice (Fig. 3).

We examined immunocytochemical and ultrastructural features of brains from several F1 generation transgenic mice from lines AE101 and AE301 at approximately 1 year of age. When sections of brain from 1-year-old control mice were stained with antibodies to the amyloid β protein (*14*), no immunoreactivity was detected (*15*). In contrast, sections of brain from transgenic mice showed amyloid β protein immunoreactivity (Fig. 3). Amyloid β protein staining was located predominantly in the hippocampus, where it appeared as clusters of dots that were symmetrically distributed on both sides of the brain. Within the hippocampus, amyloid β protein immunoreactivity was most prominent in the molecular layer of CA1 and CA2; only occasional amyloid β protein–positive clusters were detected in CA3 regions of the hippocampus and dentate gyrus. Amyloid β protein was not detected in cerebral cortex. We found similar patterns of amyloid β protein immunoreactivity in four F1 generation mice from both transgenic lines by four different amyloid β protein–specific rabbit polyclonal antibodies (*15*). Occasional clusters of amyloid β protein immunoreactivity were found in other regions of the CNS but not in a consistent pattern. Amyloid β protein immunoreactiv-

D. O. Wirak, R. Bayney, T. V. Ramabhadran, R. P. Fracasso, J. T. Hart, P. Hsiau, S. K. Pekar, G. A. Scangos, A. J. Unterbeck, Molecular Therapeutics Inc., Miles Research Center, 400 Morgan Lane, West Haven, CT 06516.
P. E. Hauer and B. D. Trapp, Department of Neurology, Johns Hopkins University School of Medicine, Baltimore, MD 21205.

*To whom correspondence should be addressed.
†Present address: Department of Molecular and Cellular Neuroscience, The Rockefeller University, New York, NY 10021.
‡Present address: Bayer AG, Pharma Research Center Aprath, D-5600 Wuppertal 1, Germany.

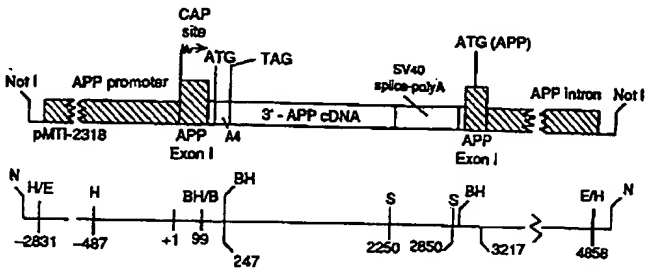


**Fig. 1.** Schematic representation of the ~7.7-kb Not I restriction fragment from pMTI-2318 (*18*) used to generate transgenic mouse lines AE101 and AE301 (*19*). A4, amyloid β protein; B, Bgl II; BH, Bam HI; E, Eco RI; H, Hind III; N, Not I; S, Sph I; BH/B, Bam HI–Bgl II fusion; and E/H or H/E, Hind III–Eco RI fusion.

ity was also associated with some but not all blood vessels in transgenic mice (Fig. 3).

Regions of hippocampus from transgenic and control mice were processed for electron microscopy (*16*). Ultrastructural correlates of the clustered dots of amyloid β protein immunoreactivity were present only in transgenic mice and consisted of intracellular accumulations of fibril-laden material (Fig. 4A) that resembled amyloid in brains from patients with AD. The cellular processes containing this amyloid-like material appeared distended, and some contained rough endoplasmic reticulum (Fig. 4B, arrows) and free ribosomes but not intermediate filament bundles (indicative of astrocytes), suggesting that they were dendrites. Amyloid-like deposits have not been detected in myelinated axons, although their presence in unmyelinated axons cannot be excluded. Ultrathin cryosections of transgenic mice hippocampus were also stained with antibodies to amyloid β protein and immunogold procedures. Gold particles in these electron micrographs were selectively enriched over the abnormal amyloid-like fibrils (*15*).

Our results illustrate that human amyloid β protein can accumulate in the CNS of transgenic mice and form amyloid-like profiles. This accumulation occurred despite low steady-state levels of amyloid β protein mRNA. Amyloid β protein deposits in postmortem brains from individuals with AD and DS are extracellular, whereas the amyloid β protein deposits in the 1-year-old transgenic mice are intracellular. Intracellular amyloid β protein immunoreactivity has also been observed in mouse hippocampal trisomy 16 grafts, a mouse model for DS (*17*). Although the source of extracellular amyloid β protein in AD is unknown, it is likely that at least a proportion of amyloid β protein has intracellular origins.

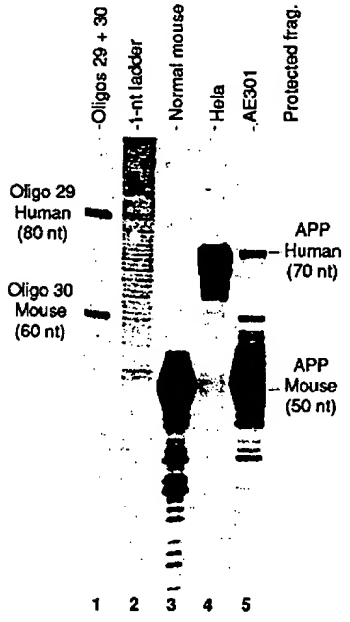


**Fig. 2.** S1 nuclease protection analysis of total RNA from normal and transgenic AE301 (F1) brain (*20*). The protected fragment sizes of the human (transgenic) and endogenous mouse APP oligonucleotide probes are 70 and 50 nucleotides (nt), respectively. Lane 1, human (oligo 29, 80 nt) and mouse (oligo 30, 60 nt) APP probes; lane 2, 1-nt DNA ladder; lane 3, normal mouse brain RNA; lane 4, Hela cell RNA; and lane 5, AE301 brain RNA. AE101, data not shown.

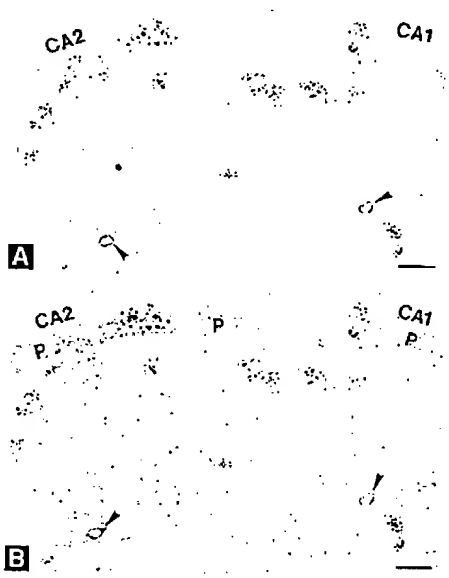


**Fig. 3.** Amyloid β protein distribution in a paraffin section from the hippocampus of a 1-year-old AE101 transgenic mouse that was photographed before (**A**) and after (**B**) hematoxylin counterstaining. Arrowheads, amyloid β protein deposits around blood vessels; and P, pyramidal cell layer of hippocampus. Scale bar: 200 μm.

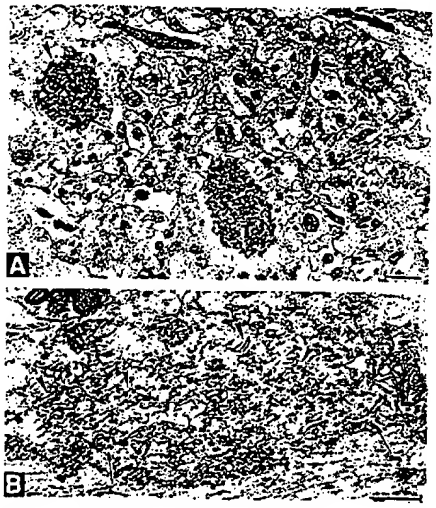


**Fig. 4.** Electron micrographs of Epon sections from the hippocampal CA1 region of a 1-year-old AE101 transgenic mouse. (**A**) Amyloid-like deposits are densely stained by uranyl acetate and lead citrate (arrowheads). (**B**) Fibrils (arrowheads) and profiles of rough endoplasmic reticulum (arrows) are associated with amyloid-like deposits. Scale bars: (A) 1.0 μm; (B) 0.5 μm.

The APP promoter is active in most neurons in the mouse CNS (*13*). The accumulation of amyloid β protein in the transgenic mice, however, is restricted primarily to the hippocampus. These data raise the possibility that amyloid β protein expression alone is not sufficient to produce amyloid-like accumulations. Although amyloid β protein–positive processes have not yet been traced to cellular perikarya, it is likely that many are dendrites of neurons concentrated in hippocampal regions CA1 and CA2. The accumulation of amyloid β protein in the CNS of these transgenic mice appears to be developmentally regulated, as it is not significant before 6 months of age (*15*). The late onset of amyloid β protein accumulation suggests that either the steady-state concentration of amyloid β protein increases with age or that factors in addition to amyloid β protein expression participate in amyloid deposition.

Evidence of neuronal cell death, early signs of neuronal degeneration, or obvious signs of CNS dysfunction have not been detected in transgenic mice at 1 year of age. Older mice will be examined for behavioral and neuropathological changes associated with amyloid β protein accumulation. The introduction of gene constructs encoding native and mutant forms of APP into transgenic mice should allow elucidation of the cellular and molecular mechanisms involved in CNS amyloidosis.

## REFERENCES AND NOTES

1. B. Muller-Hill and K. Beyreuther, *Annu. Rev. Biochem.* 58, 287 (1989); D. J. Selkoe, *Neuron* 6, 487 (1991).
2. D. Goldgaber *et al.*, *Science* 235, 877 (1987); J.

Kang *et al.*, *Nature* 325, 733 (1987); N. K. Robakis *et al.*, *Lancet* i, 384 (1987); R. E. Tanzi *et al.*, *Science* 235, 880 (1987); T. E. Golde *et al.*, *Neuron* 4, 253 (1990); A. Weidemann *et al.*, *Cell* 57, 115 (1989).
3. N. Kitaguchi *et al.*, *Nature* 331, 530 (1988); P. Ponte *et al.*, *ibid.*, p. 525; R. E. Tanzi, *ibid.*, p. 528; F. de Sauvage and J. N. Octave, *Science* 245, 651 (1989); T. E. Golde *et al.*, *Neuron* 4, 253 (1990).
4. H. G. Lemaire *et al.*, *Nucleic Acids Res.* 17, 517 (1989).
5. S. S. Sisodia *et al.*, *Science* 248, 492 (1990); F. S. Esch *et al.*, *ibid.* 248, 1122 (1990).
6. J. D. Buxbaum *et al.*, *Proc. Natl. Acad. Sci. U.S.A.* 87, 6003 (1990).
7. D. M. A. Mann and M. M. Esiri, *N. Engl. J. Med.* 318, 789 (1988); F. Tagliavani *et al.*, *Neurosci. Lett.* 93, 191 (1988); H. Yamaguchi *et al.*, *Acta Neuropathol.* 76, 541 (1988); C. L. Joachim, J. H. Morris, D. J. Selkoe, *Am. J. Pathol.* 135, 309 (1989).
8. B. A. Yankner, L. K. Duffy, D. A. Kirschner, *Science* 250, 279 (1990).
9. C. V. Broeckhoven *et al.*, *ibid.* 248, 1120 (1990); E. Levey *et al.*, *ibid.*, p. 1124.
10. A. Goate *et al.*, *Nature* 349, 704 (1991).
11. R. L. Neve, E. A. Finch, L. P. Dawes, *Neuron* 1, 669 (1988).
12. D. L. Price, *Annu. Rev. Neurosci.* 9, 489 (1986); D. J. Selkoe, *ibid.* 12, 463 (1989); L. C. Cork *et al.*, *Am. J. Pathol.* 137, 1383 (1990); L. J. Martin *et al.*, *Proc. Natl. Acad. Sci. U.S.A.* 88, 1461 (1991).
13. D. O. Wirak *et al.*, *EMBO J.* 10, 289 (1991).
14. Brains from 1-year-old AE101 and AE301 transgenic and control mice were fixed with 4% paraformaldehyde. Paraffin sections of brains were cut (8 μm thick) and immunostained by rabbit polyclonal antiserum (90-29) to the amyloid β protein (1:500 dilution) and the avidin-biotin procedure (Vector Labs, Burlingame, CA). The pattern of amyloid β protein immunoreactivity in transgenic mouse brain sections was consistent when four different rabbit polyclonal antisera directed against amyloid β protein were used. Antisera 90-25 and 90-27 were directed against amino acids 1 to 28 of amyloid β protein; antisera 90-28 and 90-29 were directed against amino acids 1 to 42. All four rabbit polyclonal antisera exhibited intense immunoreactivity with senile plaques in sections of postmortem brain from AD patients (B. D. Trapp, unpublished data). Specificity of the immunoreactivity was established by the absence of immunoprecipitate in sections stained by amyloid β protein antiserum that had been absorbed with amyloid β protein and by Western blotting.
15. B. D. Trapp, unpublished data.
16. Brains from 1-year-old AE101 transgenic and control mice were fixed with 2.5% glutaraldehyde and 4% paraformaldehyde. Ultrathin Epon sections of the hippocampus were cut, counterstained with uranyl acetate and lead citrate, and examined in a Hitachi H-600 electron microscope.
17. S.-J. Richards *et al.*, *EMBO J.* 10, 297 (1990).
18. The open reading frame for the 42-residue amyloid β protein (A4) was contained within a 148-bp Bgl II–Bam HI restriction fragment and was generated by site-directed mutagenesis [L. Kunkel *et al.*, *Methods Enzymol.* 154, 367 (1987)] of APP cDNA sequences with a synthetic oligonucleotide primer (5′-GGTGTTGTCATAGCGTAGGATCCGTCATCACCTTGGTG-3′). This Bgl II–Bam HI restriction fragment was ligated into the Bam HI site of pMTI-2307 [D. O. Wirak *et al.*, *EMBO J.* 10, 289 (1991)] to generate pMTI-2316. An ~2-kb Bam HI restriction fragment, containing APP 695 3′-end cDNA sequences, was inserted into the Bam HI site of pMTI-2316 to generate pMTI-2317. An 0.6-kb Sph I restriction fragment of pMTI-2304, containing SV40 RNA splicing signals [H. Okayama and P. Berg, *Mol. Cell. Biol.* 3, 280 (1983)] and SV40 polyadenylation signals (Bam HI–Bcl I restriction fragment from SV40 viral DNA) was ligated into a Sph I site of pMTI-2317 to generate PMTI-2318. The full-length cDNA encoding APP695 has been described [J. Kang *et al.*, *Nature* 325, 733 (1987)].
19. Transgenic mouse lines AE101 and AE301 were generated as described [D. Wirak *et al.*, *EMBO J.* 10, 289 (1991)]. In both transgenic mouse lines, multiple copies of the transgene have integrated as a head-to-tail tandem array (D. Wirak, unpublished data).
20. RNA was extracted from mouse brain and Hela cells as described [L. G. Davis, M.D. Dibner, J. F. Battey, *Basic Methods in Molecular Biology* (Elsevier, New York, 1986), pp. 130–135]. Synthetic oligonucleotides 29, 5′-GAGATAGAATACATTACTGATGTGTGGATTAATTCAAGTTCAGGCATCTACTTGTGTTACAGCACAGCTGGGCGTCCATA-3′, and 30, 5′-CGCGGGTGGGGCTTAGTTCTGCATTTGCTCAAAGAACTTGTAAGTTGGATAGGTTCCAAG-3′, were labeled with T4 polynucleotide kinase, and their specific activities were $6.04 \times 10^8$ and $5.72 \times 10^8$ cpm/μg, respectively. S1 nuclease protection analysis [S. Sisodia *et al.*, *Nucleic Acids Res.* 15, 1999 (1987)] was performed with total RNA (50 μg per sample) and 1 × $10^6$ cpm of each $^{32}$P-labeled oligonucleotide.
21. We thank C. Kundel and A. Lee for assistance in mini-gene constructions; S. Rocks and T. Garrison for transgenic animal colony management; G. Davis, T. Buckholz, and P. Tamburini for the synthesis and purification of amyloid β proteins; M. Broggi for assistance in polyclonal antibody production; P. Rae and P. Talalay for reviewing the manuscript; R. Graham for editing and typing the manuscript; C. Cootauco and E. Mulrenin for assistance in performing the morphological studies; and K.-H. Büchel for his support.

30 April 1991; accepted 20 June 1991

# Evidence for the Effects of a Superantigen in Rheumatoid Arthritis

XAVIER PALIARD, STERLING G. WEST, JOYCE A. LAFFERTY, JANICE R. CLEMENTS, JOHN W. KAPPLER, PHILIPPA MARRACK,* BRIAN L. KOTZIN*

**While studying the αβ T cell receptor repertoire in rheumatoid arthritis (RA) patients, we found that the frequency of $V_\beta14^+$ T cells was significantly higher in the synovial fluid of affected joints than in the peripheral blood. In fact, $V_\beta14^+$ T cells were virtually undetectable in the peripheral blood of a majority of these RA patients. β-chain sequences indicated that one or a few clones dominated the $V_\beta14^+$ population in the synovial fluid of individual RA patients, whereas oligoclonality was less marked for other Vβ's and for $V_\beta14$ in other types of inflammatory arthritis. These results implicate $V_\beta14$-bearing T cells in the pathology of RA. They also suggest that the etiology of RA may involve initial activation of $V_\beta14^+$ T cells by a $V_\beta14$-specific superantigen with subsequent recruitment of a few activated autoreactive $V_\beta14^+$ T cell clones to the joints while the majority of other $V_\beta14^+$ T cells disappear.**

RA IS AN AUTOIMMUNE DISEASE characterized by long-term inflammation of multiple joints. Mononuclear cell infiltration of the synovial membrane eventually can lead to the destruction of articular cartilage and surrounding structures. Because of its high frequency and potentially severe nature, this disease is a major cause of long-term disability in adults. Although the pathogenesis of RA and other similar autoimmune diseases remains unknown, genetic and environmental factors have been implicated. Several lines of evidence suggest that T cells specific for self-antigens may play a critical role in the initiation of these diseases. In the case of RA, the linkage of the disease to the DR4 and DR1 alleles of the class II genes of the major histocompatibility complex (MHC) and the finding of sometimes oligoclonal, activated $CD4^+$ T cells in synovial fluid and tissue of affected joints (*1*, *2*) suggest the involvement of $CD4^+$, αβ T cell receptor (TCR)–bearing, class II–restricted T cells in the disease. This view is supported by the finding that partial elimination or inhibition of T cells by a variety of techniques can lead to an amelioration of disease in certain patients (*3*).

Usually, potentially autoreactive T cells are deleted or inactivated by encounter with self-antigen during their development, before they can damage the individual (*4*, *5*). To understand autoimmunity one must therefore understand how self-reactive T cells escape these processes to become part of the mature T cell pool and what factors control whether these cells will remain quiescent or become activated to induce autoimmune disease. It is possible that a self-

X. Paliard, Howard Hughes Medical Institute at Denver and Department of Medicine, National Jewish Center for Immunology and Respiratory Medicine, 1400 Jackson Street, Denver, CO 80206.
S. G. West, Department of Medicine, Fitzsimons Army Medical Center, Aurora, CO 80045.
J. A. Lafferty, Department of Pediatrics, National Jewish Center, Denver, CO 80206.
J. R. Clements, Howard Hughes Medical Institute at Denver and Department of Medicine, National Jewish Center, Denver, CO 80206.
J. W. Kappler, Howard Hughes Medical Institute at Denver and Department of Medicine, National Jewish Center, Denver, CO 80206, and Departments of Microbiology/Immunology, and Medicine, University of Colorado Health Sciences Center (UCHSC), Denver, CO 80262.
P. Marrack, Howard Hughes Medical Institute at Denver and Department of Medicine, National Jewish Center, Denver, CO 80206, and Departments of Biochemistry, Biophysics, Genetics, Microbiology/Immunology, and Medicine, UCHSC, Denver, CO 80262.
B. L. Kotzin, Departments of Pediatrics and Medicine, National Jewish Center, Denver, CO 80206, and Departments of Microbiology/Immunology and Medicine, UCHSC, Denver, CO 80262.

*To whom correspondence should be addressed.

AMERICAN ASSOCIATION FOR THE ADVANCEMENT OF SCIENCE

# SCIENCE

ISSN 0036-8075
5 JULY 1991
VOLUME 253
NUMBER 5015



**ATTENTION AAAS MEMBERS**

Inside AAAS of 28 June 1991 (p. 1861) contained a preliminary list of candidates for the Association's elections for general and section officers. Additional names may be placed in nomination by petition submitted to the executive officer no later than 12 August 1991. Please refer to the 28 June issue for further details.

■ **SCIENCE (ISSN 0036-8075) is published weekly on Friday, except the last week in December, by the American Association for the Advancement of Science, 1333 H Street, NW, Washington, DC 20005.** Second-class postage (publication No. 484460) paid at Washington, DC, and additional mailing offices.  Domestic individual membership and subscription (51 issues): $82 ($50 allocated to subscription). Domestic institutional subscription (51 issues): $150. Foreign postage extra: Canada $46, other (surface mail) $46, air freight $90. First class, airmail, school-year, and student rates on request. **Change of address:** allow 6 weeks, giving old and new addresses and 11-digit account number. **Postmaster:** Send change of address to *Science*, P.O. Box 2033, Marion, OH 43305–2003. **Single copy sales:** $6.00 per issue prepaid includes surface postage; Guide to Biotechnology Products and Instruments, $20. Bulk rates on request. **Authorization to photocopy** material for internal or personal use under circumstances not falling within the fair use provisions of the Copyright Act is granted by AAAS to libraries and other users registered with the Copyright Clearance Center (CCC) Transactional Reporting Service, provided that the base fee of $1 per copy plus $0.10 per page is paid directly to CCC, 27 Congress Street, Salem, Massachusetts 01970. The identification code for *Science* is 0036-8075/83 $1 + .10. *Science* is indexed in the *Reader's Guide to Periodical Literature* and in several specialized indexes.

■ The American Association for the Advancement of Science was founded in 1848 and incorporated in 1874. Its objectives are to further the work of scientists, to facilitate cooperation among them, to foster scientific freedom and responsibility, to improve the effectiveness of science in the promotion of human welfare, to advance education in science, and to increase public understanding and appreciation of the importance and promise of the methods of science in human progress.

# EXHIBIT C

*Proc. Natl. Acad. Sci. USA*
Vol. 89, pp. 10857–10861, November 1992
Neurobiology

# Deposition of β/A4 immunoreactivity and neuronal pathology in transgenic mice expressing the carboxyl-terminal fragment of the Alzheimer amyloid precursor in the brain

ANJA KAMMESHEIDT*, FREDERICK M. BOYCE†, ATHENA F. SPANOYANNIS*, BRIAN J. CUMMINGS*, MARTA ORTEGÓN‡, CARL COTMAN*, JEFFRY L. VAUGHT‡§, AND RACHAEL L. NEVE*¶‖

*Department of Psychobiology, University of California, Irvine, CA 92717; †Division of Genetics, Children's Hospital, Boston, MA 02115; and ‡The R. W. Johnson Pharmaceutical Research Institute, Spring House, PA 19477

*Communicated by Richard F. Thompson, July 7, 1992*

**ABSTRACT** **The deposition of amyloid in senile plaques and along the walls of the cerebral vasculature is a characteristic feature of Alzheimer disease. The peptide comprising the carboxyl-terminal 100 amino acids of the β-amyloid precursor protein (βAPP) has been shown to aggregate into amyloid-like fibrils *in vitro* and to be neurotoxic, suggesting that this fragment may play a role in the etiology of Alzheimer disease. To address this question, we expressed this carboxyl-terminal 100-amino acid peptide of βAPP in transgenic mice under the control of the brain dystrophin promoter. We used an antibody to the principal component of amyloid, β/A4, to demonstrate cell-body and neuropil accumulation of β/A4 immunoreactivity in the brains of 4- and 6-month-old transgenic mice. Only light cytoplasmic staining with this antibody was visible in control mice. In addition, immunocytochemical analysis of the brains with an antibody to the carboxyl terminus of βAPP revealed abnormal aggregation of this epitope of βAPP within vesicular structures in the cytoplasm and in abnormal-appearing neurites in the CA2/3 region of the hippocampus in transgenic mice, similar to its aggregation in the cells of Alzheimer disease brains. Thioflavin S histochemistry suggested accumulations of amyloid in the cerebrovasculature of transgenic mice with the highest expression of the βAPP-C100 transgene. These observations suggest that expression of abnormal carboxyl-terminal subfragments of βAPP *in vivo* may cause amyloidogenesis and specific neuropathology.**

Alzheimer disease (AD) is a neurodegenerative disorder characterized by progressive loss of memory and declining cognitive function beginning in late life. A prominent feature of AD neuropathology is the deposition of amyloid in senile plaques and along the walls of the cerebrovasculature. The peptide fragment termed β/A4 (39–43 amino acids; refs. 1 and 2) is the principal constituent of the amyloid deposits, although plaques contain numerous other components. The β-amyloid protein precursor (βAPP), from which β/A4 is derived, is a transmembrane protein in which the β/A4 peptide spans the border between the extracellular domain and the transmembrane region (3, 4). Normal cleavage of βAPP in the secretory pathway occurs at the β/A4 $Lys^{16}$-$Leu^{17}$ peptide bond (5). Recent data, however, have revealed that multiple β/A4-containing carboxyl-terminal fragments of βAPP are also produced in the brain, via the endosomal–lysosomal system (6).

Additional evidence has implicated at least one of these fragments, the carboxyl-terminal 100 amino acids of βAPP, in the development of AD neuropathology. This fragment, which spans the β/A4 and cytoplasmic domains, is amyloidogenic (7–9) and neurotoxic both *in vitro* (10, 11) and *in vivo* (12). To test the hypothesis that this neurotoxic fragment may play a role both in amyloidogenesis and in the development of the progressive neuropathology of AD, we introduced into mice a transgene carrying the sequence for the carboxyl-terminal 104 amino acids of βAPP (βAPP-C104) under control of the brain dystrophin promoter (13). Both founders and $F_1$ transgenic progeny manifested (*i*) accumulation of β/A4 immunoreactive material in neuronal cell bodies and (*ii*) a subcellular shift of immunoreactivity for the carboxyl terminus of βAPP from its normal distribution throughout the cell soma to aggregates in the cytoplasm and the neuropil in the hippocampus. Mice in three of the nine lines examined, with the most robust transgene expression in the brain, displayed accumulation of β/A4 immunoreactivity in abnormal-appearing neurites, as well as thioflavin S-fluorescent deposits in the cerebrovasculature. These neuropathological features were not seen in control mice.

## METHODS

**Production of Transgenic Mice.** The *Bgl* II–*Sma* I fragment of the βAPP-695 cDNA [base pairs (bp) 1769–2959] was cloned into a modified form of plasmid pRSV in which the Rous sarcoma virus promoter was replaced with the dystrophin neural promoter (13). The βAPP-C104 transgene, together with the upstream dystrophin promoter and the downstream simian virus 40 splice and polyadenylylation sequences, was excised from plasmid sequences by digestion with *Mlu* I and *Bam*HI and was microinjected into the pronuclei of fertilized eggs from $F_2$ hybrid mice (C57BL/6 × SJL) at the National Transgenic Development Facility (DNX, Princeton, NJ). The injected mouse eggs were reimplanted into pseudopregnant recipient females.

**Immunochemical and Histologic Analysis of Transgenic and Control Mice.** Fourteen $F_1$ backcross progeny from six different founder lines (ages, 3.5–4 months) and founders only from three additional lines (ages, 6 months) were analyzed histologically. We also analyzed 8 age-matched C57BL/6 and SJL controls. All 22 mice were subjected to each immunocytochemical and histological analysis.

E1-42 immunocytochemistry on mouse and human sections and F5 immunocytochemistry on human sections were carried out as described by Cummings *et al.* (14). F5 and F8 immunocytochemistry on mouse brains was carried out as described by Neve *et al.* (12). All comparisons of transgenic and control mice were made using tissue processed in parallel and developed with diaminobenzidine for equivalent periods

The publication costs of this article were defrayed in part by page charge payment. This article must therefore be hereby marked "*advertisement*" in accordance with 18 U.S.C. §1734 solely to indicate this fact.

Abbreviations: AD, Alzheimer disease; βAPP, β-amyloid protein precursor.

§Present address: Cephalon, Inc., West Chester, PA 19380.
¶Present address: Molecular Neurogenetics Laboratory, McLean Hospital, Belmont, MA 02178.
‖To whom reprint requests should be addressed.

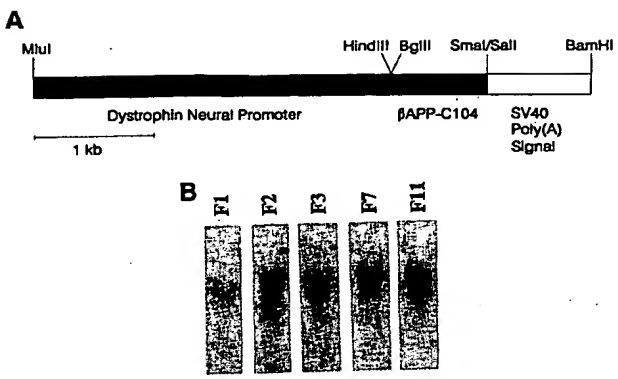


FIG. 1. (*A*) Schematic of the brain dystrophin promoter–βAPP-C104 fusion transgene. SV40, simian virus 40. (*B*) Southern blot analysis of selected transgenic lines.

of time. Sections incubated in parallel without E1-42, F5, or F8 primary antibody failed to develop any staining.

Sections subjected to thioflavin S histochemistry were incubated for 20 min in 1:1 absolute ethanol/chloroform and then rinsed three times for 1 min in 95% ethanol, 3 min in 70% ethanol, 3 min in 50% ethanol, and 3 min in water. Sections were then incubated for 4 min with 1% (wt/vol) thioflavin S (Sigma) in water and differentiated in 80% ethanol.

## RESULTS

**Characterization of Transgenic Mice Carrying the βAPP-C104 cDNA Under Control of the Dystrophin Brain Promoter.** We anticipated that the low level of transcripts controlled by the dystrophin brain promoter might be important in allowing survival of βAPP-C104 transgenic mice beyond the embryonic stage. Hence, a 4.65-kilobase (kb) DNA fragment containing a dystrophin brain promoter–βAPP-C104 fusion gene with the simian virus 40 early-region splice and polyadenylylation sequences (Fig. 1*A*) was isolated and microinjected into the male pronuclei of fertilized eggs from $F_2$ hybrid mice

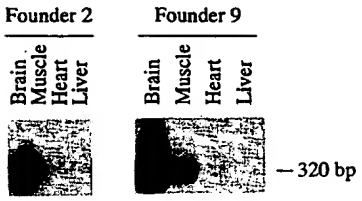


FIG. 2. Predominant brain expression of the βAPP-C104 transgene is revealed by reverse transcription–PCR. Hybridization of a radiolabeled interior oligonucleotide to a Southern blot of the amplification products from four tissue RNAs in two of the transgenic lines is shown.

(C57BL/6 × SJL). PCR analysis of tail DNA from 36 offspring revealed that 12 of the mice were positive for the transgene; 10 survived for further analysis. We used Southern blot analysis to estimate the transgene copy number in *Bam*HI-digested DNA from each founder line (representative lanes are shown in Fig. 1*B*). Positively hybridizing bands exceeded 20 kb in all founder lines, indicating incorporation of the transgene into the mouse genome (*Bam*HI does not cleave within the transgene). Copy number of the transgene ranged from 1 (line 4) to >20 (lines 2, 7, and 11). Seven founder mice produced transgenic offspring in crosses with normal C57BL/6 mice, and Southern blot analysis of selected $F_1$ and $F_2$ progeny showed that the transgenic DNA was inherited with no observable rearrangements or changes in copy number (data not shown).

**Expression of the βAPP-C104 Transgene Predominantly in the Brain.** We analyzed RNA from brain, skeletal muscle, heart, and liver of $F_1$ transgenic progeny from six founders at the age of 4 months and from the three founder mice that did not produce offspring when they reached the age of 6 months. Reverse transcription was coupled with PCR as described (15) to amplify a 320-bp segment of the transgene RNA (Fig. 2) and revealed that predominant expression of the transgene occurred in the brain. Highest expression was seen in lines 2, 3, 4, and 7. Although the transgene was transcribed at low levels in other tissues in some of the lines, in all transgenic

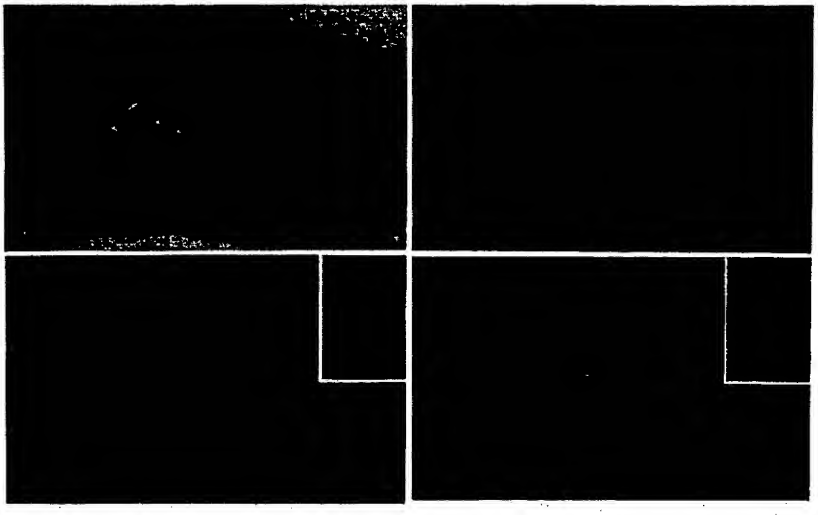

FIG. 3. (*A* and *B*) E1-42 immunoreactivity in the hippocampus of a transgenic mouse (*A*), compared with that of a control mouse (*B*). While low-level staining of cell bodies in the pyramidal cell layer and in additional scattered cells is seen in the control mouse (*B*), darker punctate accumulations of E1-42 immunoreactivity in the pyramidal cell layer (*A*, arrow) and throughout the hippocampus (*A*) are unique to the transgenic mice. Higher magnifications of the punctate intracellular deposits of E1-42 immunoreactivity in transgenic animals are shown in Fig. 4. (*C* and *D*) E1-42 immunoreactivity in the parietal cortex of a transgenic mouse (*C*) and a control mouse (*D*). Differences in E1-42 immunoreactivity between transgenic and control mice in the parietal cortex are much less pronounced than in the hippocampus. Preabsorption of the E1-42 antibody with 30 μg of peptide per μl of antibody resulted in absence of staining (*Insets*). (Bars = 100 μm.)

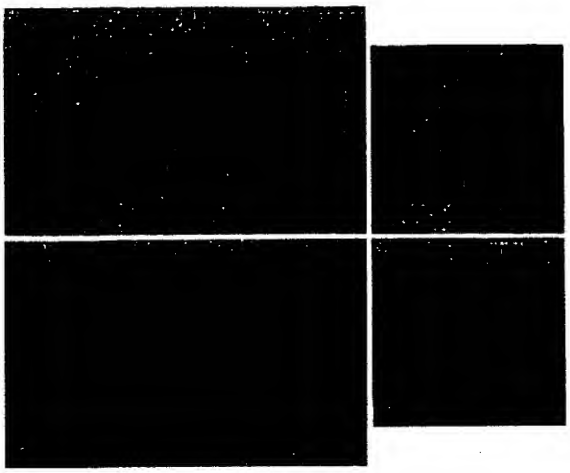

FIG. 4. High-power depictions of the punctate intracellular deposits of E1-42 immunoreactivity in transgenic mouse (*A* and *C*), and comparison with control (*B* and *D*). Note the darkly staining intracellular aggregates of E1-42 immunoreactivity in the hippocampus of transgenic mouse (*A*, arrowheads); increased magnification of one of these aggregates is shown in *C*. In contrast, E1-42 immunoreactivity appears as pale homogeneous cytoplasmic staining in some hippocampal neurons (*B*, arrowheads); a more-strongly stained neuron is shown at higher power in *D*. Note the lack of punctate accumulations of E1-42 immunoreactivity in these cells. (Bars = 10 μm.)

animals its expression was ≥10 times higher in brain than in any other tissue examined.

**Analysis of β/A4 Immunoreactivity in the Brains of the Transgenic Mice.** We used an affinity-purified polyclonal antibody, E1-42, raised against a peptide representing the 42-amino acid β/A4 fragment, to detect β/A4 epitopes in the transgenic mouse brains. This antibody does not immunostain normal βAPP in the human brain but is specific for amyloid cores in the neuritic plaques, as well as diffuse amyloid deposits that are not detectable by conventional histological stains for amyloid, such as thioflavin S (14). Immunostaining of control mouse brains with E1-42 was slightly different from that of control human brains, in that it showed very pale homogeneous staining of cell bodies in all nontransgenic mice (Fig. 3*B*; Fig. 4 *B* and *D*). In contrast, immunostaining of the brains of 4-month-old $F_1$ transgenic mice from six lines, and of three 6-month-old founder mice, revealed abnormal intraneuronal β/A4 immunoreactivity throughout the brain in all of the transgenic mice. The strongest E1-42 immunopositive cells, however, predominated in the hippocampus [Fig. 3*A*; compare with E1-42 immunoreactivity in the parietal cortex, which is very similar between transgenic (Fig. 3*C*) and control (Fig. 3*D*) animals]. Preabsorption of the E1-42 antibody with the β/A4 peptide resulted in loss of specific staining (*Insets*, Fig. 3 *C* and *D*). In most cases, the E1-42 immunoreactivity occurred as punctate deposits within neurons that had a rounded, compact appearance (Fig. 4 *A* and *C*). The intracellular accumulation of β/A4 immunoreactivity was particularly prominent within the hilus (Fig. 5), and close examination of the E1-42 staining in this region showed that the immunoreactivity extended beyond the cell body, with punctate deposits visible in some processes (Fig. 5*B*). Deposits of β/A4 immunoreactivity were not visible in the hilus of control animals (Fig. 5*C*) and did not resemble the age-associated inclusions in normal and transgenic C57BL/6J mice that are occasional immunocytochemical artifacts (16).

Transgenic mice of lines 2, 3, and 7, with the most robust transgene expression in the brain, displayed punctate accumulations of β/A4 immunoreactivity in short, somewhat

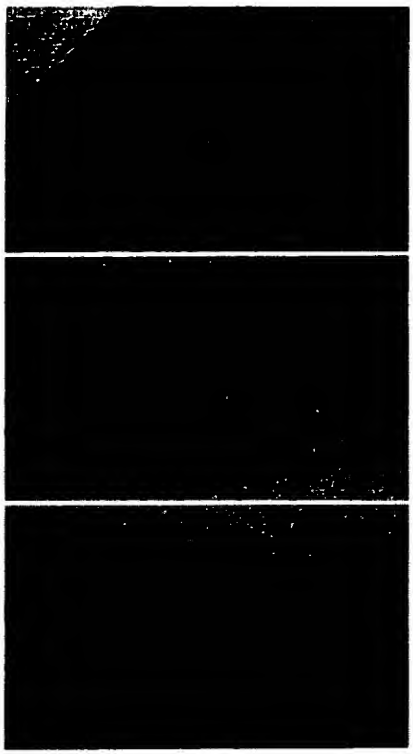

FIG. 5. E1-42 immunoreactivity in the hilus of a transgenic mouse (*A* and *B*), compared with that of a control mouse (*C*). This region of the hippocampus possessed the highest density of cells with intracellular β/A4 immunoreactive deposits (*A*); punctate deposits are also visible in the neuropil (*B*). An enlargement of the field outlined in *A* is depicted in *B*. A comparable enlargement of the hilar field of a control animal is depicted in *C*. (Bars = 100 μm.)

curly, abnormal-appearing fibers that were apparent in the stratum radiatum of the CA2/3 region of the hippocampus (Fig. 6), similar to the accumulations shown in Fig. 5 in the hilus. The emergence of E1-42 immunoreactivity in the neuropil may represent a later stage of amyloid deposition or pathology than that seen in the cell soma, since it was

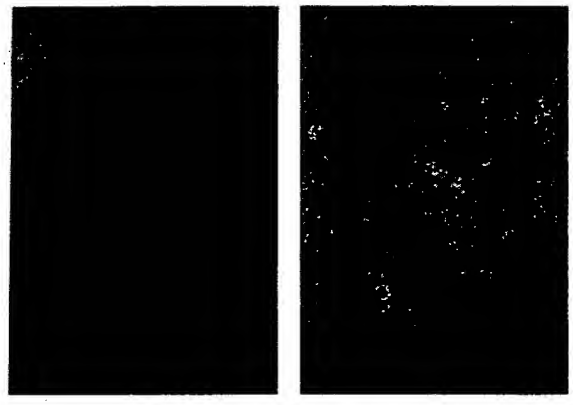

FIG. 6. E1-42 immunoreactivity in the neuropil at the CA2/3 boundary in a transgenic mouse with a high copy number of the transgene. Punctate β/A4 deposits have virtually disappeared from cell bodies of this region in this mouse and are instead found accumulated in curly dystrophic-appearing fibers throughout the area (*A*). A greater magnification of a sector of the region displayed in *A* is shown in *B*. (Bar in *A* = 100 μm; bar in *B* = 10 μm.)

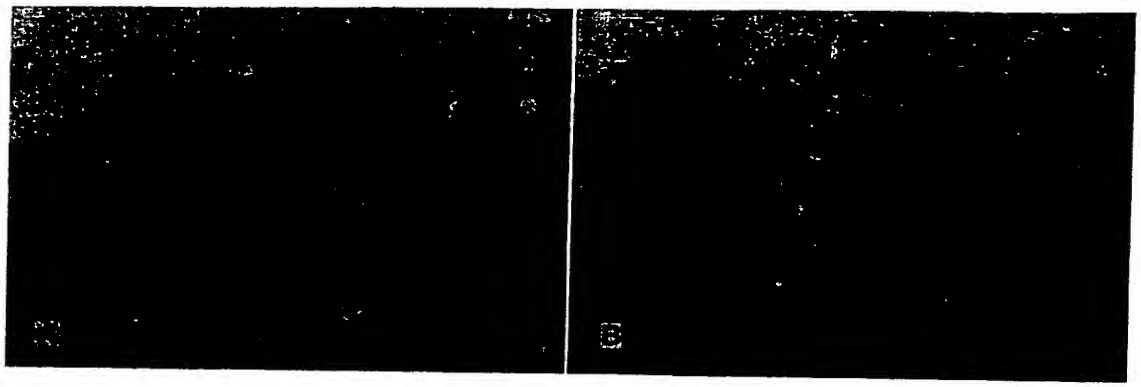

FIG. 7. F5 immunostaining of transgenic (*A*) and control (*B*) animals at the CA2/3 boundary in the hippocampus. Note that the F5 epitope (the carboxyl terminus of βAPP) has accumulated in punctate vesicular structures within the cell somata and has collected in the neuropil in the transgenic animal. (Bars = 10 μm.)

confined to those mouse lines with the highest transgene expression and was never seen in controls.

**Subcellular Shift of the βAPP Carboxyl Terminus.** Previous work showed that immunoreactivity for the carboxyl-terminal epitope of βAPP segregated into enlarged intracellular organelles in the hippocampus in AD (17) and highlighted neuropil aberrations in the hippocampus of mice transplanted with transfected PC12 cells expressing βAPP-C104 (12). We detected a similar phenomenon in the transgenic mice. Staining of the brain sections with F5, an antibody to the carboxyl-terminal 9 amino acids of βAPP (17), showed a striking change in the subcellular localization of the F5 epitope, which was particularly evident in the CA2/3 region of the hippocampus in transgenic mice. Whereas control mice displayed homogeneous F5 staining predominantly of the neuronal somata in this region (Fig. 7*B*), the F5 immunoreactivity in the transgenic mice took on a punctate appearance in the cell somata (Fig. 7*A*). This punctate staining, which often extended markedly into the neuronal processes, was also revealed with an independent antibody to the carboxyl terminus of βAPP (F8; data not shown). Adjacent Nissl-stained sections did not reveal detectable gross morphological abnormalities in the area of altered F5 staining, suggesting that the intracellular disorganization of the F5 epitope does not reflect cell body degeneration in transgenic mice of this age.

In mice from lines 2, 3, and 7, with highest transgene expression in the brain, the cells in the hippocampal region showed particularly dense reaction product in the neuropil, and the F5 reactivity in the soma took the form of larger accumulations, as if the punctate vesicular immunoreactive material was fusing or aggregating (Fig. 8*A*). The distribution of the F5 immunoreactivity in these cells was very similar to its distribution in CA1 hippocampal neurons in human AD brains (Fig. 8*C* and ref. 17) relative to controls (Fig. 8*D*). The similarity in the appearance of the punctate cell-body F5 immunoreactivity in transgenic animals and in AD individuals in the hippocampus is marked (Fig. 8 *A* and *C*), and is suggestive of an early stage of pathology.

**Cerebrovascular Staining of Transgenic Mice with Thioflavin S.** The mice from lines 2, 3, and 7, with the highest brain expression of the transgene, displayed thioflavin S fluorescence associated with blood vessels (Fig. 9), which we also observed in AD brains stained with thioflavin S. This fluorescence suggested that amyloid had accumulated in or around the cerebral blood vessels of these transgenic animals.

## DISCUSSION

We have shown that expression of βAPP-C104 in the brains of transgenic mice can lead to the deposition of intracellular

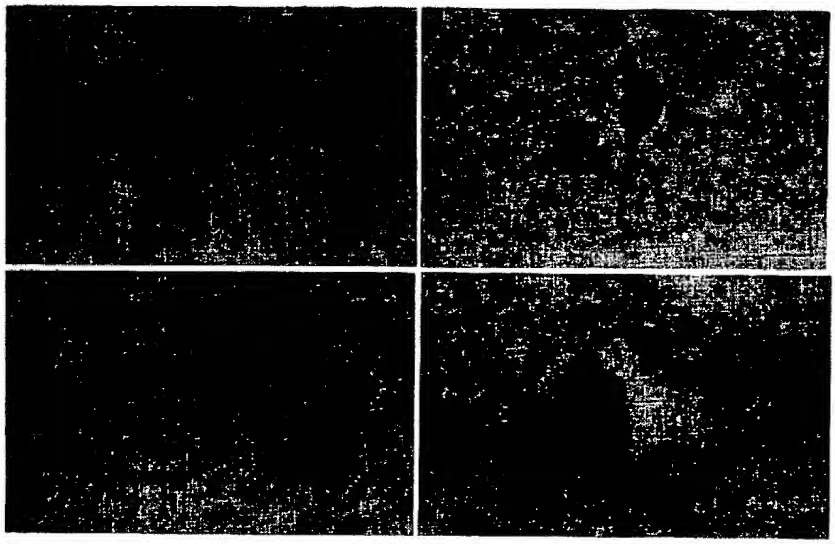

FIG. 8. (*A* and *C*) Cytoplasmic accumulations of the F5 epitope in hippocampal pyramidal cells of a transgenic mouse and a human AD brain, respectively. (*B* and *D*) F5 immunostaining of hippocampal pyramidal cells in a control mouse and a control human brain, respectively. (Bars = 10 μm.)

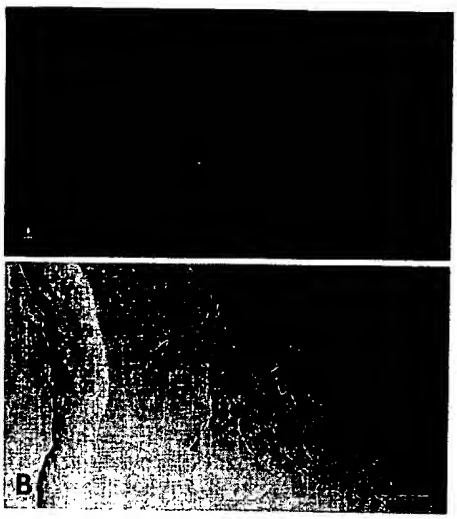

FIG. 9. (*A*) Thioflavin S fluorescence around blood vessels in the hippocampus of a transgenic mouse from line 2. (*B*) Thioflavin S-positive structures correlate with blood vessels as shown with Nomarsky optics (arrowheads). (Bars = 100 μm.)

β/A4 immunoreactivity and cerebrovascular amyloid, as well as early neuronal pathology as manifested by abnormal intracellular accumulations of the carboxyl-terminal epitope of βAPP, some of which occurred in dystrophic-appearing neurites. Interestingly, Quon *et al.* (18) also detected abnormal neurites with punctate accumulations of β/A4 immunoreactivity in transgenic mice overexpressing βAPP-751.

Previous work has shown that the enlarged intracellular organelles into which the F5 immunoreactivity segregates in AD, similar to those we observed in the transgenic mice, are probably fused lysosomes (17). The dense F5 immunostaining in these enlarged organelles was particularly prominent in regions of the hippocampus that were heavily invested with pathology, such as CA1, in which the heavy staining of the pyramidal cells was accompanied by atrophy of many of these cells (18). Although Nissl and Bielschowsky stains did not reveal gross neuronal death in any of the transgenic brains, it is possible that accumulation of the F5 epitope in enlarged lysosomes may presage neuronal degeneration.

We do not know whether the F5 immunoreactivity that aggregates into cellular compartments in the transgenic mice reflects the presence of only the carboxyl terminus of βAPP in the swollen organelles or also the larger precursor protein. An antibody to protease nexin II (the extracellular secreted portion of βAPP) detects enlarged punctate accumulations of βAPP within degenerating neurons and dystrophic neurites, as well as within plaques, in AD brain (14). These observations suggest that the compartmentalization of βAPP, presumably into lysosomes, during the disease process is not limited to the carboxyl terminus of the molecule. These data, coupled with those of Cataldo and Nixon (19), Joachim *et al.* (20), and Golde *et al.* (6), also imply that the generation of amyloid deposits is not exclusively an extracellular process and may in fact begin within the neuron.

Thioflavin S-positive material was observed in the cerebrovasculature of three of the transgenic animals. This material was not immunoreactive with E1-42, which is consistent with the failure of this antibody to detect thioflavin S-positive cerebrovascular amyloid in AD brain. During the analyses of the βAPP-C104 transgenic mice, we tested five additional β/A4 antibodies, all of which stained plaque amyloid in AD brain and punctate intracellular deposits in the transgenic mice without staining cerebrovascular amyloid in either AD brain or the mouse brains. Recent data (21) indicate that there are conformational differences in β/A4 derived from plaque and cerebrovascular amyloid, respectively. Moreover, thioflavin S is a stain that defines the structure termed amyloid, which includes the deposits found in various peripheral amyloidoses as well as those detected in cerebral amyloideses (22). While β/A4 is the principal component of amyloid in AD, other molecules contribute in varying degrees to the formation of this thioflavin S-positive structure and may constitute a relatively large percentage of this structure in the cerebrovasculature of the transgenic mice.

These βAPP-C104 mice may provide a model for dissecting the molecular events that lead to the accumulation of amyloid and possibly neurodegeneration in AD brain and may be useful for developing therapeutic agents that can halt or reverse these processes.

We appreciate the many helpful discussions we had with Drs. K. Kosik and R. Nixon. We thank Dr. P. Brandt for computer help with the figures, Dr. K. Ivins for help with perfusing the mice, Dr. D. Schenk for the F5 and F8 antibodies, Dr. M. Rosenberg for the simplified protocol for extraction of tail DNA, and J. Zimmerman for making human AD and age-matched control tissue available to us. We acknowledge National Institute of Child Health and Human Development Contract NO1-HD-0-2911 in support of DNX, Inc., as the source of the transgenic mice. This research was supported by Contract 90-00198 from the California State Department of Health Services, a Focused Giving grant from Johnson & Johnson, a Metropolitan Life Foundation Award, and National Institutes of Health Grants HD18658 and NS28406 (R.L.N.). F.M.B. is the Betty Banker Fellow of the Muscular Dystrophy Association.

1. Glenner, G. G. & Wong, C. W. (1984) *Biochem. Biophys. Res. Commun.* **120**, 885–890.
2. Masters, C. L., Simms, G., Weinman, N. A., Multhaup, G., McDonald, B. L. & Beyreuther, K. (1985) *Proc. Natl. Acad. Sci. USA* **82**, 4245–4249.
3. Weidemann, A., Konig, G., Bunke, D., Fischer, P., Salbaum, J. M., Masters, C. L. & Beyreuther, K. (1989) *Cell* **57**, 115–126.
4. Selkoe, D. J., Podlisny, M. B., Joachim, C. L., Vickers, E. A., Lee, G., Fritz, L. C. & Oltersdorf, T. (1988) *Proc. Natl. Acad. Sci. USA* **85**, 7341–7345.
5. Anderson, J. P., Esch, F. S., Keim, P. S., Sambamurti, K., Lieberburg, I. & Robakis, N. K. (1991) *Neurosci. Lett.* **128**, 126–128.
6. Golde, T. E., Estus, S., Younkin, L. H., Selkoe, D. J. & Younkin, S. G. (1992) *Science* **255**, 728–730.
7. Dyrks, T., Weidemann, A., Multhaup, G., Salbaum, J. M., Lemaire, H.-G., Kang, J., Müller-Hill, B., Masters, C. L. & Beyreuther, K. (1988) *EMBO J.* **7**, 949–957.
8. Wolf, D., Quon, D., Wang, Y. & Cordell, B. (1990) *EMBO J.* **9**, 2079–2084.
9. Maruyama, K., Terakado, K., Usami, M. & Yoshikawa, K. (1990) *Nature (London)* **347**, 566–569.
10. Yankner, B. A., Dawes, L. R., Fisher, S., Villa-Komaroff, L., Oster-Granite, M. L. & Neve, R. L. (1989) *Science* **245**, 417–420.
11. Kozlowski, M. R., Spanoyannis, A., Manly, S. P., Fidel, S. A. & Neve, R. L. (1992) *J. Neurosci.* **12**, 1679–1687.
12. Neve, R. L., Kammesheidt, A. & Hohmann, C. F. (1992) *Proc. Natl. Acad. Sci. USA* **89**, 3448–3452.
13. Boyce, F. M., Beggs, A. H., Feener, C. & Kunkel, L. M. (1991) *Proc. Natl. Acad. Sci. USA* **88**, 1276–1280.
14. Cummings, B. J., Su, J. H., Geddes, J. W., Van Nostrand, W. E., Wagner, S. L., Cunningham, D. D. & Cotman, C. W. (1992) *Neuroscience* **48**, 763–777.
15. Brandt, P., Neve, R. L., Kammesheidt, A., Rhoads, R. E. & Vanaman, T. C. (1992) *J. Biol. Chem.* **267**, 4376–4385.
16. Jucker, M., Walker, L. C., Martin, L. J., Kitt, C. A., Kleinman, H. K., Ingram, D. K. & Price, D. L. (1992) *Science* **255**, 1443–1445.
17. Benowitz, L. I., Rodriguez, W., Paskevich, P., Mufson, E. J., Schenk, D. & Neve, R. L. (1989) *Exp. Neurol.* **106**, 237–250.
18. Quon, D., Wang, Y., Catalano, R., Marian Scardina, J., Murakami, K. & Cordell, B. (1991) *Nature (London)* **352**, 239–241.
19. Cataldo, A. M. & Nixon, R. A. (1990) *Proc. Natl. Acad. Sci. USA* **87**, 3861–3865.
20. Joachim, C., Games, D., Morris, J., Ward, P., Frenkel, D. & Selkoe, D. (1991) *Am. J. Pathol.* **138**, 373–384.
21. Barrow, C. J. & Zagorski, M. G. (1991) *Science* **253**, 179–182.
22. Cohen, A. S. (1986) in *Amyloidosis*, eds. Marrink, J. & Van Rijswijk, M. H. (Nihjoff, Dordrecht), pp. 3–19.

# EXHIBIT D

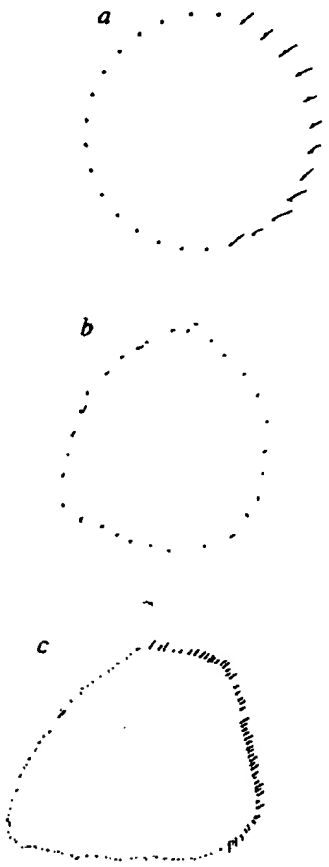


FIG. 4 J.R.'s attempts to cancel the local components of a predrawn figure (*a*); to reproduce the figure (*b*); and to draw the figure and then cancel its local components (*c*).

even when focal attention cannot be automatically directed to local components on the left of a global figure. J.R.'s neglect is thus neither purely perceptual nor purely motor; it rather arises from an input-deficit to a 'premotor' mechanism[10] committed to the exogenous control of focal attention. Lesions that 'disrupt the cross-talk between inferior posterior areas' can reduce or eliminate interactions between global and local processing[9]. Whether this disruption in J.R. is due solely to her right hemisphere lesion (or also implicates her left thalamic infarct) is unclear. One further problem remains: why is J.R. unaware of the discrepancy between her global percepts and local actions? The process of local completion can mask perceptual incongruity but cannot then control appropriate manual output. J.R. can perceive the whole forest but cannot use that percept to search for and cut down the trees on the left thereof. □

Received 6 September; accepted 12 December 1994.

1. Marshall, J. C. & Halligan, P. W. *Nature* **336**, 766–787 (1988).
2. Halligan, P. W. & Marshall, J. C. *Cogn. Neuropsychol.* **11**, 167–206 (1994).
3. Navon, D. *Cogn. Psychol.* **9**, 353–383 (1977).
4. Sergent, J. *Brain* **111**, 347–373 (1988).
5. Bottini, G., Sterzi, R. & Vallar, G. *J Neurol. Neurosurg. Psychiat.* **55**, 562–565 (1992).
6. Halligan, P. W. & Marshall, J. C. *Cortex* **30**, 685–694 (1994).
7. Kinsbourne, M. *Trans. Am. Neurol. Assoc.* **95**, 143–145 (1970).
8. Ladavas, E., Del Pesce, M., Mangun, G. R. & Gazzaniga, M. S. *Cogn. Neuropsychol.* **11**, 57–74 (1994).
9. Robertson, L. C. in *Cognitive Neuropsychology in Clinical Practice* (ed. Margolin, D. I.) 70–95 (Oxford University Press, New York, 1992).
10. Rizzolatti, G. & Berti, A. *Rev. Neurol.* **146**, 626–634 (1990).

ACKNOWLEDGEMENTS. This work was supported by the Medical Research Council.

# Alzheimer-type neuropathology in transgenic mice overexpressing V717F β-amyloid precursor protein

**Dora Games*, David Adams†‡, Ree Alessandrini†, Robin Barbour*, Patricia Berthelette†‡, Catherine Blackwell†‡, Tony Carr*, James Clemens§, Thomas Donaldson†‡, Frances Gillespie†‡, Terry Guido*, Stephanie Hagopian†‡, Kelly Johnson-Wood*, Karen Khan*, Mike Lee*, Paul Leibowitz†‡, Ivan Lieberburg*¶, Sheila Little§, Eliezer Masliah‖, Lisa McConlogue*, Martin Montoya-Zavala†‡, Lennart Mucke☆, Lisa Paganini*, Elizabeth Penniman†, Mike Power*, Dale Schenk*, Peter Seubert*, Ben Snyder†, Ferdie Soriano*, Hua Tan*, James Vitale†‡, Sam Wadsworth†‡, Ben Wolozin** & Jun Zhao***

* Athena Neurosciences, Inc., 800 Gateway Boulevard, South San Francisco, California 94080, USA
† Exemplar Corporation, One Innovation Drive, Worcester, Massachusetts 01605, USA
§ Lilly Research Laboratories, Indianapolis, Indiana 46285, USA
☆ The Scripps Research Institute, Department of Neuropharmacology, 10666 North Torrey Pines Road, La Jolla, California 92037, USA
‖ Department of Neurosciences, University of California, San Diego, 9500 Gilman Drive, La Jolla, California 92093, USA
** Laboratory of Clinical Science, National Institute of Mental Health, 9000 Rockville Pike, 1013D41, Bethesda, Maryland 20892, USA

ALZHEIMER'S disease (AD) is the most common cause of progressive intellectual failure in aged humans. AD brains contain numerous amyloid plaques surrounded by dystrophic neurites, and show profound synaptic loss, neurofibrillary tangle formation and gliosis. The amyloid plaques are composed of amyloid β-peptide (Aβ), a 40–42-amino-acid fragment of the β-amyloid precursor protein (APP)[1]. A primary pathogenic role for APP/Aβ is suggested by missense mutations in APP that are tightly linked to autosomal dominant forms of AD[2,3]. A major obstacle to elucidating and treating AD has been the lack of an animal model. Animals transgenic for APP have previously failed to show extensive AD-type neuropathology[4–10], but we now report the production of transgenic mice that express high levels of human mutant APP (with valine at residue 717 substituted by phenylalanine) and which progressively develop many of the pathological hallmarks of AD, including numerous extracellular thioflavin S-positive Aβ deposits, neuritic plaques, synaptic loss, astrocytosis and microgliosis. These mice support a primary role for APP/Aβ in the genesis of AD and could provide a preclinical model for testing therapeutic drugs.

Transgenic mice were generated using a platelet-derived growth factor (PDGF)-$\beta$ promoter[11] driving a human APP (hAPP) minigene encoding the $APP_{717V\rightarrow F}$ mutation associated with familial AD[12] (PD-APP; Fig. 1*a*). The construct contained APP introns 6–8, allowing alternative splicing of exons 7 and 8.

‡ Present addresses: Department of Biology and Biotechnology, Worcester Polytechnic Institute, 100 Institute Road, Worcester, MA 01609, USA (D.A.); Genzyme Corporation, One Mountain Road, Framingham, MA 01701, USA (P.B.); University of Massachusetts, Department of Veterinarian and Animal Sciences, Amherst, MA 01003, USA (C.B.); Molecular Therapeutics Inc, 400 Morgan Lane, West Haven, CT 06516, USA (T.D.); Transkaryotic Therapies Inc., 195 Albany Street, Cambridge, MA 02139, USA (F.G.); Joint Program in Neonatology, Children's Hospital, Enders, Rm 950, 300 Longwood Avenue, Boston, MA 02115, USA (S.H.); Innovir Laboratories Inc., 510 East 73 Street, New York, NY 10022, USA (P.L.); Alteon Inc., 170 Williams Drive, Ramsey, NJ 07446, USA (M.M.-Z.); Millennium Pharmaceuticals Inc., 640 Memorial Drive, Cambridge, MA 02139, USA (J.V.).
¶ To whom correspondence should be addressed.

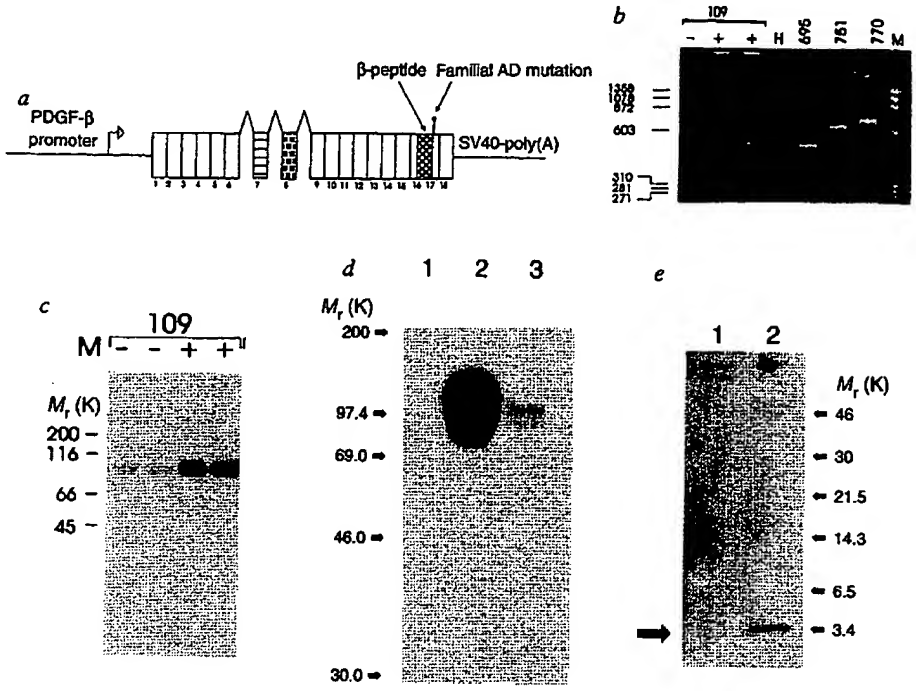


Fig. 1 analysis of app expression in brain tissue of pd-app transgenic mice. *a*, Map of the APP construct (PD-APP) minigene used to generate transgenic mice (not to scale). The construct contains the PDGF $\beta$-chain promoter, full-length hAPP cDNA encoding the Val-to-Phe mutation at codon 717, and the inclusion of genomic sequences for hAPP introns 6–8. *b*, RT-PCR analysis demonstrates the presence of transcripts encoding the 695, 751 and 770 isoforms of hAPP in transgenic animal brains (+) but not in brains from non-transgenic littermates (−). Control reactions using human brain RNA (H) as well as cDNA clones encoding hAPP 695, 751 or 770 are also shown. M, Markers (calibration in bp). *c*, Immunoblot analysis of total APP expression (human and mouse) in transgenic mouse (+) and control littermate (−) brain tissue using a C-terminal APP antibody, $\alpha$6. *d*, Human-specific APP expression in brain tissue from a 6-month-old non-transgenic littermate (lane 1), transgenic mouse (lane 2) or human AD cortex (lane 3) using immunoblotting with the human-specific APP antibody 8E5. *e*, Immunoprecipitation and immunoblot analysis of A$\beta$ from the brain tissue of a 9-month-old non-transgenic littermate (lane 1) and a 9-month-old transgenic mouse (lane 2).

METHODS. The PDGF $\beta$-chain 5′ flanking sequence included 1.3 kb upstream of the transcription initiation site and ~70 bp of 5′ untranslated region, ending at the *Aur*II site[10]. The $\beta$-APP sequences were derived from human $\beta$-APP cDNA starting with the *Nru*I site in exon 1 through to the end of exon 6 and from the beginning of exon 9 through to exon 18, including the 3′ untranslated sequence ending at the *Sph*I site, and from human genomic sequences from exons 6–9, including all intervening introns. To introduce the familial AD mutation at position 717, Val was mutated to Phe (G to T, using the P-Select mutagenesis kit; Promega). The late SV40 polyadenylation signal was provided by the 240-bp *Bam*HI to *Bcl*I fragment. Plasmid sequences (pUC) were removed by *Sac*1 and *Not*1 digestion before microinjection. Transgenic mice were generated using standard techniques[19], except that PD-APP DNA was microinjected into the embryos at the two-cell stage. Seven founder mice were generated and line 109 was used for extensive analysis. RNA was isolated from brain tissue as described[20] and subjected to RT-PCR as described[21] using human-specific APP primers (5′-CCGATGATGACGAGGACGAT-3′, 5′-TGAACACGTGACGAGGCCGA-3′) with the following PCR conditions: 40 cycles of 1 min at 94 °C, 40 s at 60 °C, 50 s at 72 °C. The identities of the human APP RT-PCR bands from the transgenic mouse RNA were verified by subcloning and sequencing. Analysis of holo-APP involved brain homogenization in 10 volumes of PBS containing 0.5 mM EDTA, 10 μg ml$^{-1}$ leupeptin and 1 mM PMSF. Samples were spun at 12,000*g* for 10 min and the pellets resuspended in RIPA (150 mM NaCl, 50 mM Tris, pH 8.0, 20 mM EDTA, 1.0% deoxycholate, 1.0% Triton X-100, 0.1% SDS, 1 mM PMSF and 10 μg ml$^{-1}$ leupeptin (*d*)). Samples (each containing 30 μg total protein) were analysed by SDS–PAGE, transferred to Immobilon and reacted with either the holo-APP antibody, $\alpha$6 (ref. 22), or 8E5 monoclonal antibody. 8E5 was prepared against a bacterial fusion protein encompassing hAPP residues 444–592 (ref. 22) and is human-specific showing essentially no crossreactivity against mouse APP (*d*, lane 1). For immunoblot analysis of A$\beta$ (*e*), a 9-month-old mouse brain was homogenized in 5 ml 6 M guanidine HCl, 50 mM Tris, pH 7.5. The homogenate was centrifuged at 100,000*g* for 15 min and the supernatant was dialysed against $H_2O$ overnight adjusted to PBS with 1 mM PMSF and 25 μg ml$^{-1}$ leupeptin. This material was immunoprecipated with antibody 266 resin, and immunoblotted with the human-specific A$\beta$ antibody, 6C6, as described[13].

We used only heterozygous animals. Southern analysis of 104 from four generations showed that ~40 copies of the transgene were inserted at a single site and transmitted in a stable manner (data not shown). Human APP messenger RNA was produced in several tissues of the transgenic mouse, but at especially high levels in brain (not shown). RNase protection assays revealed ~18-fold more APP expression in the brains of line 109 animals than in most previously described lines expressing neuron-specific enolase (NSE)-promoter-driven APP transgenes (not shown; refs 4, 8–10). In addition, the three major splicing variants of hAPP mRNA (695, 751, 770)[1] were expressed in the transgenic mice, as evidenced by reverse-transcriptase polymerase chain reaction (RT-PCR) (Fig. 1*b*). Immunoblot analysis of brain homogenates using either a holo-APP polyclonal antibody or a human-specific APP monoclonal antibody revealed hAPP overexpression in the transgenic mouse at levels ≥10-fold higher than either endogenous mouse APP levels (Fig. 1*c*, *d*) or those in AD brain (Fig. 1*d*). Using human-specific A$\beta$ antibodies, we isolated a 4K A$\beta$-immunoreactive peptide from the brains of the transgenic animals, which corresponds to the relative molecular mass of A$\beta$ (Fig. 1*e*). Brain levels of A$\beta$ were at least 10-fold higher in line-109 animals than in the previously described hAPP transgenic mice (not shown; ref. 9). Finally, embryonic day-16 cortical cell cultures from transgenic animals constitutively secreted human A$\beta$, including a substantial fraction of A$\beta$ 1–42 (5 ng ml$^{-1}$ total A$\beta$; 0.7 ng ml$^{-1}$ A$\beta$ 1–42), as detected in media by human-specific A$\beta$ enzyme-linked immunosorbent assays (not shown; refs 9 and 13). Thus, line-109 animals greatly overexpressed human APP mRNA, holo-APP and A$\beta$ in their brains.

Brains from 18 transgenic animals and 12 age-matched non-transgenic littermate controls (4–13 months old) representing three generations of the line-109 pedigree were extensively examined histopathologically. Between 4–6 months of age ($n$=7), no obvious pathology was detected; however, at ~6–9 months of age ($n$=7), transgenic animals began to exhibit deposits of human A$\beta$ in the hippocampus, corpus callosum and cerebral cortex, but not in other brain regions. These increased with age, and by eight months many deposits (30–200 μm) were seen (Fig. 2*a*). As the animals aged (≥9 months; $n$=4), the density of the plaques increased (Fig. 2*c*) until the A$\beta$-staining pattern resembled that of AD (Fig. 2*a*, inset). Robust pathology was

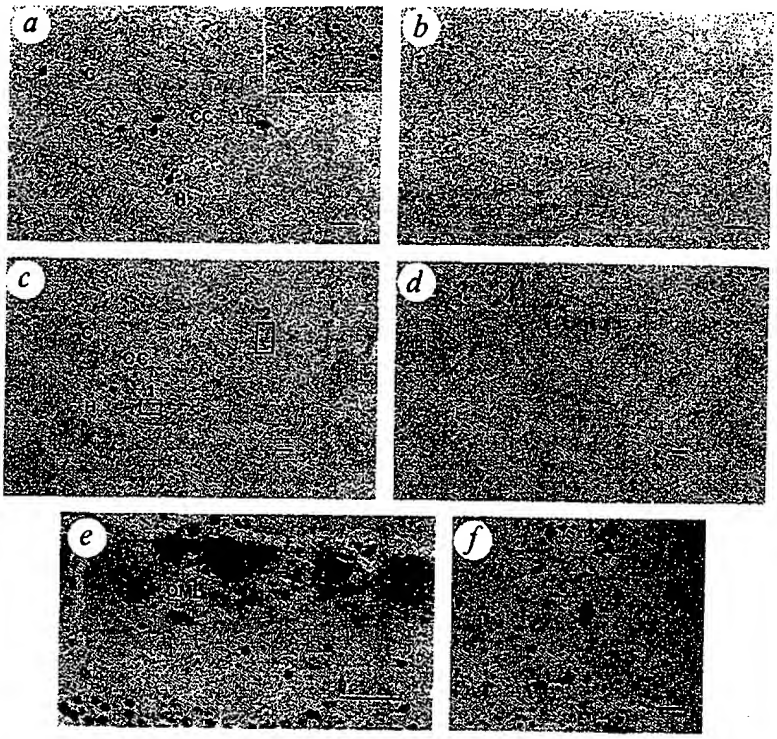


FIG. 2 Demonstration of AD-like amyloid plaques in PD-APP transgenic mice. Human and mouse brain sections were labelled with antiserum R1280 generated against synthetic human Aβ 1–40 peptide. H, Hippocampus; C, cortex; CC, corpus callosum; OML, outer molecular layer of the dentate gyrus; F, hippocampal fissure. Coronal sections of the hippocampus and neocortex from *a*, an 8-month-old transgenic mouse containing Aβ deposits (arrows), and *b*, a non-transgenic littermate. Inset in *a*, human tissue from AD frontal cortex stained with R1280. Adjacent parasaggital sections from a 13-month-old transgenic mouse before (*c*) and after (*d*) preincubation of the antibody with synthetic Aβ 1–40 peptide. In *c*, the large increase in Aβ was confined to the cortex and hippocampus. Several regions of the hippocampus contained densely packed Aβ, including the terminal zone of the perforant pathway in the outer molecular layer of the dentate gyrus (arrowheads). Boxed areas 1 and 2 are shown at higher magnification in *e* and *f*, respectively. Scale bars in *a–d*, 200 μm. In *e*, the outer molecular layer of the dentate gyrus contained areas of compacted and diffuse (asterisk) plaques. The edge of the granule cell layer is visible at the bottom. In *f*, a field of Aβ deposits in the occipital cortex. Scale bars in *e* and *f*, 40 μm.

METHODS. Mouse brains were removed and placed in Trojanowski's fixative[23] for 48 h before paraffin embedding. 6-μm coronal or parasaggital sections from transgenic and non-transgenic mice were placed adjacent to each other on poly-L-lysine coated slides. Sections were deparaffinized, rehydrated, and treated with 0.03% $H_2O_2$ for 30 min before overnight incubation at 4 °C with a 1:1,000 dilution of the Aβ antibody, R1280 (ref. 24). For absorption studies, synthetic human Aβ 1–40 peptide[25] in 10% aqueous dimethylsulphoxide was added to a final concentration of 7.0 μM to the diluted antibody and incubated for 2 h at 37 °C. The diluent was applied to the sections and processed under the same conditions as the standard antibody solution. Peroxidase rabbit IgG kit (Vector Labs) was then used as recommended, with 3,3'-diaminobenzidine (DAB) as the chromagen. Similarly fixed human AD brain was processed simultaneously under identical conditions.

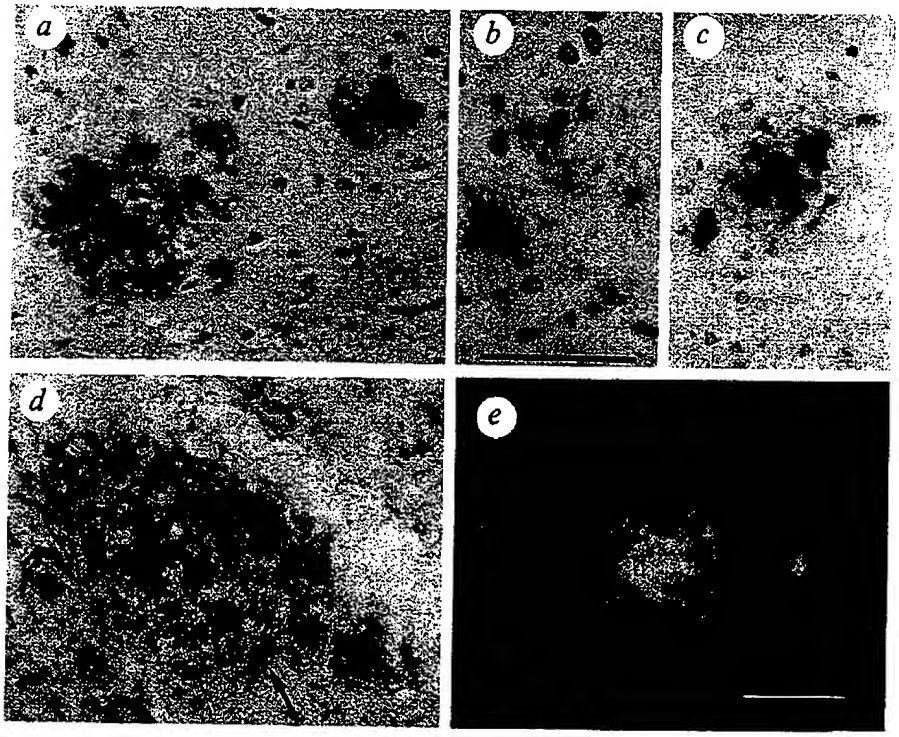


FIG. 3 Morphological diversity of Aβ deposition in the PD-APP mouse brain. Roughly spherical (*a*), and wispy, irregular deposits (*b*), labelled with antibody 9204 (Aβ1–5; ref. 26) specific for the free N terminus of Aβ. *c*, Aβ core and surround labelled with antibody 277-2, specific for the C terminus of Aβ1–42. *d*, Astrocytic gliosis (arrow) associated with Aβ deposition was evident after double immunolabelling with antibodies to glial fibrillary acidic protein (GFAP, red) and human Aβ (Aβ 1–5; brown). *e*, Aβ deposits were also reactive with thioflavin S. A compacted Aβ core and 'halo' is evident in the large plaque. The fine background fluorescence represents autofluorescent lipofuscin granules. Scale bars, 50 μm.

METHODS. For *a–c*, immunochemistry was performed as described for Fig. 2. Antibody 9204 (to Aβ1–5) was used at a concentration of 7.0 μg $ml^{-1}$. Antibody 277-2, specific for Aβ1–42 (apparent affinity for Aβ1–42 = 75 nM versus >10 μM for Aβ1–40 by radioimmunoassay competition), was prepared by immunizing New Zealand white rabbits with the peptide cysteine-aminoheptanoic acid–Aβ33–42 conjugated to cationized BSA ('Super Carriers'; Pierce) using a typical immunization protocol (500 μg per injection). Specific antibodies were affinity-purified from serum against the immunogen immobilized on agarose beads. Before incubation with 277-2 (10 μg $ml^{-1}$) sections were treated for 1–2 min with 80% formic acid. In *c*, the antibody 9204 was reacted using the peroxidase rabbit IgG kit (Vector Labs). The product was then visualized with DAB, and the sections were incubated overnight at 4 °C with a 1:500 dilution of polyclonal anti-GFAP (Sigma). The GFAP antibody was reacted using the alkaline phosphatase anti-rabbit IgG kit and alkaline phosphatase substrate kit I, (Vector Labs; used according to the manufacturer's recommendations). Sections were stained with thioflavin S using standard procedures[27] and viewed with ultraviolet light through an FITC filter of maximum wavelength 440 nm.

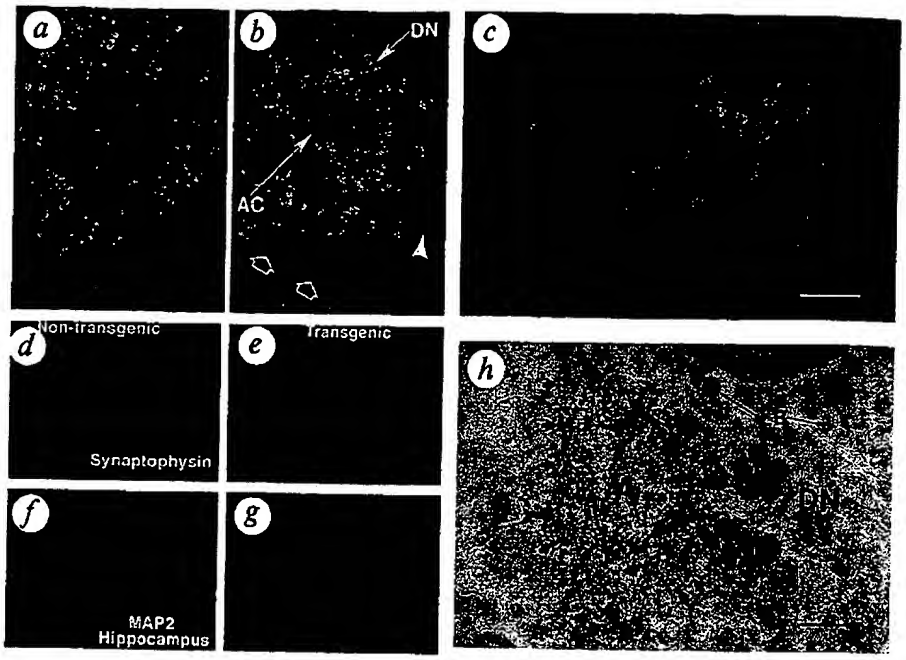


FIG. 4 Laser scanning confocal images of human and 8-month-old transgenic mouse brains, demonstrating the relationship of extracellular cortical Aβ deposit to dystrophic neurites and neuropil abnormalities, as well as the reduction of synaptic density and dendrites in the transgenic hippocampus. An Aβ deposit and adjacent neuropil in an 8-month-old transgenic mouse brain are also shown in an electron micrograph. In both human (*a*) and mouse (*b*) brains, Aβ deposits (red) were associated with distorted neurites (DN) containing synaptophysin (green). Yellow signifies overlap of the two markers. *b*, Aβ immunoreactive plaque in a transgenic mouse brain containing a central amyloid core (AC); synaptic loss (arrowhead) and compression (open arrows) of the neuropil surrounding the amyloid deposit are also evident. *c*, Aβ deposit (red) in a transgenic mouse brain associated with morphologically abnormal hAPP-positive neurites (green). The magnification for *a–g* is indicated by the scale bar in c (20 μm). Both synaptophysin (red) and microtubule-associated protein-2 (MAP-2; green) immunostaining were reduced throughout the molecular layer of the hippocampal dentate gyrus in the transgenic mouse (*e*, *g*) compared to the non-transgenic littermate (*d*, *f*). *h*, Immunoelectron micrograph of a transgenic mouse brain demonstrating extracellular Aβ deposition (A) decorated with the human-specific R1280 Aβ antiserum (outlined by arrows). A dystrophic neurite (DN) in the immediate vicinity of the Aβ deposit contained abundant large mitochondria (M) and laminar dense bodies (LB). Scale bar, 2 μm.

METHODS. 40-μm-thick vibratome sections were incubated overnight at 4 °C with the following antibodies: R1280 (1:1,000) in combination with polyclonal anti-synaptophysin in *a* and *b* (1:150; Dako) or 8E5 in c (7.0 μg ml$^{-1}$; described in Fig. 1). For *d–g*, sections were incubated with anti-synaptophysin or monoclonal anti-MAP 2 (1:20, Boehringer-Mannheim), and reacted with a goat anti-rabbit biotinylated antibody (1:100) followed by a mixture of FITC-conjugated horse anti-mouse IgG (1:75) and avidin D Texas red (1:100) (Vector Labs). The double-immunolabelled sections were viewed on a Zeiss Axiovert 35 microscope with attached laser confocal scanning system MRC 600 (Bio-Rad). The Texas red channel collected images of the R1280 (*a*, *b*, *c*) or synaptophysin (*d*, *e*) labelling, and the FITC channel collected synaptophysin (*a*, *b*), 8E5 (*c*), or MAP 2 (*f*, *g*) labelling. Optical *z*-sections 0.5 μm in thickness were collected from each region; details of similar image processing and storage are described in ref. 28. For immunoelectron microscopy, mice were perfused with saline followed by 2.0% paraformaldehyde and 1.0% glutaraldehyde in cacodylate buffer. 40-μm-thick vibratome sections were incubated with R1280, and reacted as in Fig 2. Immunolabelled sections with Aβ deposits were then fixed in 1.0% ammonium tetraoxide and embedded in epon/araldite before viewing ultrathin sections with a Jeol CX100 electron microscope[29].

also seen in another transgenic line generated from the PD-APP vector (line 35; data not shown). Aβ deposits of varying morphology clearly were evident as a result of using a variety of Aβ antibodies, including well characterized human-specific Aβ antibodies (Figs 2, 3) and antibodies specific for the free amino and carboxy termini of Aβ 1–42 (Fig. 3*a–c*). Serial sections demonstrated many plaques were positively stained with both of the latter antibodies. The forms of the Aβ deposition ranged from diffuse irregular types to compacted plaques with cores (Fig. 3). Non-transgenic littermates (Fig. 2*b*) showed none of these neuropathological changes. Immunostaining was fully absorbable with the relevant synthetic peptide (Fig. 2*d*), and was apparent using a variety of processing conditions, including fixation with paraformaldehyde and Trojanowski methods (Figs 2, 3). Many plaques were stained with thioflavin S (Fig. 3*e*), and some were also stained using the Bielschowsky silver method and were birefringent with Congo red (not shown), indicating the true amyloid nature of these deposits. Confirmation of the presence of extracellular Aβ was obtained using immunoelectron microscopy (Fig. 4*h*). The majority of plaques were intimately surrounded by GFAP-positive reactive astrocytes (Fig. 3*d*), similar to the gliosis found in AD plaques. The neocortices of the transgenic mice contained diffusely activated microglial cells, as defined by their amoeboid appearance and shortened processes (not shown). Preliminary attempts to identify neurofibrillary tangles with tau antibodies were negative, consistent with their well known absence in rodent tissues[14]. Nevertheless, clear evidence for neuritic pathology was apparent using both conventional and confocal immunomicroscopy. Many Aβ plaques were closely associated with distorted neurites that could be detected with hAPP-specific antibodies (Fig. 4*c*) and with anti-synaptophysin antibodies (Fig. 4*b*), suggesting that these neurites were derived in part from axonal sprouts, as observed in the AD brain (Fig 4*a*). The plaques compressed and distorted the surrounding neuropil (Fig. 4*b*), also as in the AD brain (Fig. 4*a*). Finally, synaptic and dendritic density were reduced in the molecular layer of the hippocampal dentate gyrus of the transgenic mice. This was evident by reduced immunostaining for the presynaptic marker synaptophysin (compare Fig. 4*d* and *e*) and the dendritic marker MAP-2 (compare Fig. 4*f* and *g*), as described in AD brain[15].

Several transgenic rodent lines have been produced that express either the hAPP gene or hAPP complementary DNAs regulated by a variety of promoters[4–10]. In particular, NSE-driven $APP_{751}$ transgenic mice[9,10] have sparse Aβ deposits which are more typical of early AD and young Down's syndrome cases; in these mice, unlike ours, mature lesions such as frequent compacted plaques, neuritic dystrophy and extensive gliosis were very rare[10]. Our success in generating AD-like pathology consistently in these transgenic mice is probably due to the construct used and the high level of hAPP expression. The transgene contains a splicing cassette that permits expression of all three major hAPP isoforms. Expression is driven by the PDGF-β promoter, which is known to target expression preferentially to neurons

of the cortex, hippocampus, hypothalamus and cerebellum of transgenic animals[11]. The familial AD mutation at residue 717[12] may be important as it partially shifts production of Aβ from the 40-amino-acid form to the more amyloidogenic 42-residue peptide known to predominate in plaques[16,17]. Preparation of APP transgenic mice independently harbouring each of these features will be required to identify the essential component(s) that result in pathology.

The most notable feature of these transgenic mice is their Alzheimer-like neuropathology, which includes extracellular Aβ deposition, dystrophic neuritic components, gliosis and loss of synaptic density with regional specificity resembling that of AD. Based on the limited sampling to date, plaque density appears to increase with age in these transgenic mice, as it does in humans[1], implying a progressive Aβ deposition that exceeds its clearance, as also proposed for AD[18]. Our transgenic model provides strong new evidence for the primacy of APP expression and Aβ deposition in AD neuropathology and offers a means to test whether compounds that lower Aβ production and/or reduce its neurotoxicity *in vitro* can produce beneficial effects in an animal model prior to advancing such drugs into human trials. □

Received 17 October 1994; accepted 5 January 1995.

1. Selkoe, D. J. *A. Rev. Neurosci.* **17**, 489–517 (1994).
2. Hardy, *J. Clin. geriatr. Med.* **10**, 239–247 (1994).
3. Mann, D. M. A. *et al. Neurodegeneration* **1**, 201–215 (1992).
4. Quon, D. *et al. Nature* **352**, 239–241 (1991).
5. Sanhu, F. A., Salim, M. & Zain, S. B. *J. biol. Chem.* **266**, 21331–21334 (1991).
6. Lamb, B. T. *et al. Nature Genet.* **5**, 22–30 (1993).
7. Pearson, B. E. & Choi, T. K. *Proc. natn. acad. Sci. U.S.A.* **90**, 10578–10582 (1993).
8. Mucke, L. *et al. Brain Res.* **668**, 151–167 (1994).
9. McConlogue, L. *et al. Neurobiol. Aging* **15**, S12 (1994).
10. Higgins, L. S. *et al. Ann. Neurol.* **35**, 598–607 (1994).
11. Sasahara, M. *et al. Cell* **64**, 217–227 (1991).
12. Murrell, J. *et al. Science* **254**, 97–99 (1991).
13. Seubert, P. *et al. Nature* **359**, 325–327 (1992).
14. Cork, L. C. *et al. J. Neuropath. exp. Neurol.* **47**, 629–641 (1988).
15. Masliah, E. *et al. Am. J. Path.* **138**, 235–246 (1991).
16. Suzuki, N. *et al. Science* **264**, 1336–1340 (1994).
17. Roher, A. *et al. J. biol. Chem.* **269**, 3072–3083 (1993).
18. Maggio, J. E. *et al. Proc. natn Acad. Sci. U.S.A.* **89**, 5462–5466 (1992).
19. Hogan, B., Constantini, F. & Lacey, E. In *Manipulating the Mouse Embryo: A Laboratory Manual* (Cold Spring Harbor Laboratory, Cold Spring Harbor, NY, 1986).
20. Chomazynski, P. & Sacchi, N. *Analyt. Biochem.* **162**, 156–159 (1987).
21. Wang, A. M. *et al. Proc. natn. Acad. Sci. U.S.A.* **86**, 9717–9721 (1989).
22. Oltersdorf, T. *et al. J. biol. Chem.* **265**, 4492–4497 (1990).
23. Aral, H. *et al. Proc. natn. Acad. Sci. U.S.A.* **87**, 2249–2253 (1990).
24. Tamaoka, A. *et al. Proc. natn. Acad. Sci. U.S.A.* **89**, 1345–1349 (1992).
25. Games, D. *et al. Neurobiol. Aging* **13**, 569–576 (1992).
26. Saido, T. C. *et al. J. biol. Chem.* **269**, 15253–15257 (1994).
27. Dickson, D. W. *et al. Acta neuropath.* **79**, 486–493 (1990).
28. Masliah, E. *et al. J. Neuropath. exp. Neurol.* **52**, 619–632 (1993).
29. Masliah, E. *et al. Acta neuropath.* **81**, 428–433 (1991).

ACKNOWLEDGEMENTS. We thank M. Mallory, A. Maya, N. Ge, E. Rockenstein, O. Stephenson and E. Johnstone for technical assistance; the animal care technicians involved in this project; J. Trojanowski for human brain sections; T. Saido and D. Selkoe for anti-Aβ antibodies 9204 and R1280, respectively; T. Collins and D. Goldgaber for the PDGF promoter and APP cDNA subclones, respectively; and D. Selkoe for helpful comments and advice.

# Gating of the voltage-dependent chloride channel ClC-0 by the permeant anion

**Michael Pusch, Uwe Ludewig, Annett Rehfeldt* & Thomas J. Jentsch†**

Centre for Molecular Neurobiology (ZMNH), Hamburg University, Martinistrasse 52, D-20246 Hamburg, Germany

**CHLORIDE channels of the ClC family are important for the control of membrane excitability[1–3], cell volume regulation[4,5], and possibly transepithelial transport[6,7]. Although lacking the typical voltage-sensor found in cation channels[8–10], gating of ClC channels is clearly voltage-dependent. For the prototype *Torpedo* channel ClC-0 (refs 11–15) we now show that channel opening is strongly facilitated by external chloride. Other less permeable anions can substitute for chloride with less efficiency. ClC-0 conductance shows an anomalous mole fraction behaviour with $Cl^-/NO_3^-$ mixtures, suggesting a multi-ion pore. Gating shows a similar anomalous behaviour, tightly linking permeation to gating. Eliminating a positive charge at the cytoplasmic end of domain D12 changes kinetics, concentration dependence and halide selectivity of gating, and alters pore properties such as ion selectivity, single-channel conductance and rectification. Taken together, our results strongly suggest that in these channels voltage-dependent gating is conferred by the permeating ion itself, acting as the gating charge.**

The *Torpedo* electric organ $Cl^-$-channel ClC-0 (ref. 12) has a 'slow' gate operating on both protochannels of the double-barrelled channel[13,14] simultaneously, and a 'fast' gate acting on single protochannels[13–15]. Both gates have opposite voltage-dependence, with the fast gate being opened by depolarization. ClC-0 was expressed in *Xenopus* oocytes and the fast gate was studied in isolation (Fig. 1*a*). The dependence of the steady-state open probability, $p_{open}$, on the transmembrane voltage $V$ can be described by the Boltzmann distribution $p_{open} = 1/(1+\exp(z_n e_0(V_{1/2}-V)/kT))$ (where $e_0$ is the elementary charge, $V_{1/2}$ is the voltage of half-maximal activation, $k$ is the Boltzmann constant, and $T$ is the temperature) with a nominal gating charge $z_n \sim 1$ in agreement with earlier data[13,14]. Consistent with single-channel measurements[13,14], gating kinetics indicate a two-state gating mechanism. Reducing extracellular $Cl^-$ concentration ($[Cl^-]_o$) shifts $p_{open}(V)$ to positive voltages without significantly changing its slope (the gating charge) (Fig. 1*b*). In contrast, intracellular chloride has little effect (Fig. 1*c*). A dependence of ClC-0 microscopic gating transitions on the $Cl^-$-gradient has already been noted[15].

The dependence of gating on $[Cl^-]_o$ could be due to a simple mechanism in which channel opening depends on chloride binding to a site within the pore; $p_{open}$ should then increase with $[Cl^-]_o$ and with positive intracellular potentials. Intracellular chloride has little effect on gating, because it cannot reach its binding site in the closed state.

The simplest model assumes that chloride-binding to a single site in the pore is required for channel opening[10]. Although it may serve as a first approximation to our data, the shift of $p_{open}$ with $[Cl^-]_o$ is ~20% less than minimally predicted[10]. This suggests that this model is either principally unsuited to explain ClC-0 gating, or that it needs further refinement.

The pores of many channels, including certain chloride channels[16], can accommodate more than one ion, leading to concentration-dependent interactions within the pore. In a single-ion pore, conductance changes monotonously when the concentration ratio between two permeant ionic species is varied; in a multi-ion pore, however, interactions between different species can lead to a current minimum at a certain concentration ratio, an 'anomalous mole fraction behaviour'[16,17]. We indeed found this effect with mixtures of $Cl^-$ and $NO_3^-$ (Fig. 2*b*), indicating that ClC-0 has a multi-ion pore. Thus, a model having a single chloride-binding site[10] may be too simplistic.

* Deceased.
† To whom correspondence should be addressed.

9 Feb 1995 Vol. 373 Issue no. 6514

## ON THE COVER

**A mouse model for Alzheimer's**
Pages 523 and 476

**Structure of a DNA repair enzyme**
Page 487

**The trouble with gas giants**
Pages 494 and 470

**An isotopic puzzle**
Page 496

Nature Publishing Company

◀ The lack of an animal model has been hampered research into the pathogenesis of Alzheimer's disease. Previous efforts to transfer the human β-amyloid precursor protein (APP) into mice have failed to produce the characteristic amyloid plaque pathology, but the mice described on page 523 express high levels of a mutant APP, display amyloid plaques, and develop many other signs characteristic of Alzheimer's. Cover shows confocal image of plaque with reactive gliosis. See News and Views page 476.

## THIS WEEK...

### DNA repair kit

Uracil–DNA glycosylases are responsible for initiating repair of uracil residues in DNA, one of the commonest forms of mutagenic lesion, and the report of the three-dimensional structure of such an enzyme throws light on the structural basis of DNA damage repair. The structure of herpes simplex virus uracil–DNA glycosylase alone, and in complexes with uracil base and with an oligonucleotide, suggests binding models for both single- and double-stranded substrates. Page 487.

### Gas giants an endangered species?

Are 'gas-giant' planets such as Jupiter and Saturn rarities? Only relatively young stars are surrounded by the large quantities of gas that are required to form gas giants, so by the $10^7$ years or so required for planet formation according to current models, much of the gas will have escaped. Direct observations of molecular gas around stars in the critical age range of $10^6$–$10^7$ years now show that after only a few million years, the gas remaining is insufficient to make a Jupiter-size planet. Planet formation must accordingly be much quicker than present models suggest. Pages 494 and 470.

### Isotopic puzzle from space

Primitive meteorites are isotopically heterogeneous, reflecting the composition of material from the Solar System. Planetary or asteroidal material, however, has been thermally 'processed' and is expected to be isotopically homogeneous. The Acapulco meteorite is a fragment of an asteroidal body that has experienced heating and partial melting, yet, as El Goresy *et al.* report, it includes graphite grains retaining the isotopic signatures of a diverse range of precursor materials. Page 496.

### Caucasus race

The discovery in Dmanisi, East Georgia, of the well preserved fossil jawbone of an early human has aroused great interest because the region is a possible 'gateway to Europe', where *Homo erectus* was suspected but not documented. A fossil mandible (right), found in 1991, is now described in detail (pages 509 and 472); it is the earliest example of *H. erectus* to be found in western Eurasia (1.6–1.8 million years old) and shows similarities to African and Chinese members of the species.

## OPINION



## NEWS



## CORRESPONDENCE



## NEWS AND VIEWS



*Nature*® (ISSN 0028-0836) is published weekly on Thursday, except the last week in December, by Macmillan Magazines Ltd (4 Little Essex Street, London WC2R 3LF). Annual subscription for USA and Canada US$425 (institutional/corporate), US$135 (individual making personal payment). US and Canadian orders to: *Nature*, Subscription Dept, PO Box 1733, Riverton, NJ 08077-7333, USA. Other orders to *Nature*, Brunel Road, Basingstoke, Hants RG21 2XS, UK. Second class postage paid at New York, NY 10012, and additional mailing offices. Authorization to photocopy material for internal or personal use, or internal or personal use of specific clients, is granted by *Nature* to libraries and others registered with the Copyright Clearance Centre (CCC) Transactional Reporting Service, provided the base fee of $9.00 an article (or $1.00 a page) is paid direct to CCC, 27 Congress Street, Salem, MA 01970, USA. Identification code for *Nature*: 0028-0836/95 $9.00+$1.00. US Postmaster send address changes to: Nature, 65 Bleecker Street, New York, NY 10012. Published in Japan by Nature Japan K.K., Shin-Mitsuke Bldg. 36 Ichigaya Tamachi, Shinjuku-ku, Tokyo 162, Japan. 

# EXHIBIT E

*Proc. Natl. Acad. Sci. USA*
Vol. 94, pp. 1550–1555, February 1997
Neurobiology

# Amyloid precursor protein processing and $A\beta_{42}$ deposition in a transgenic mouse model of Alzheimer disease

**(PDAPP mouse/β-peptide/amyloidogenesis)**

K. JOHNSON-WOOD, M. LEE, R. MOTTER, K. HU, G. GORDON, R. BARBOUR, K. KHAN, M. GORDON, H. TAN, D. GAMES, I. LIEBERBURG, D. SCHENK, P. SEUBERT*, AND L. MCCONLOGUE

Athena Neurosciences, Inc., 800 Gateway Boulevard, South San Francisco, CA 94080

*Communicated by L. Iversen, University of Oxford, Oxford, United Kingdom, December 6, 1996 (received for review August 18, 1996)*

ABSTRACT **The PDAPP transgenic mouse, which overexpresses human amyloid precursor protein (APP717V→F), has been shown to develop much of the pathology associated with Alzheimer disease. In this report, levels of APP and its amyloidogenic metabolites were measured in brain regions of transgenic mice between 4 and 18 months of age. While absolute levels of APP expression likely contribute to the rate of amyloid β-peptide (Aβ) deposition, regionally specific factors also seem important, as homozygotic mice express APP levels in pathologically unaffected regions in excess of that measured in certain amyloid plaque-prone regions of heterozygotic mice. Regional levels of APP and APP-β were nearly constant at all ages, while Aβ levels dramatically and predictably increased in brain regions undergoing histochemically confirmed amyloidosis, most notably in the cortex and hippocampus. In hippocampus, Aβ concentrations increase 17-fold between the ages of 4 and 8 months, and by 18 months of age are over 500-fold that at 4 months, reaching an average level in excess of 20 nmol of Aβ per g of tissue. $A\beta_{1-42}$ constitutes the vast majority of the depositing Aβ species. The similarities observed between the PDAPP mouse and human Alzheimer disease with regard to $A\beta_{42}$ deposition occurring in a temporally and regionally specific fashion further validate the use of the model in understanding processes related to the disease.**

In the Alzheimer disease (AD) brain, region-specific amyloid β-peptide (Aβ) amyloidosis is a key pathological feature and is accompanied by astrogliosis, microgliosis, cytoskeletal changes, and synaptic loss. These pathological alterations are thought to be linked to the cognitive decline that clinically defines the disease (1). AD primarily afflicts the elderly, although genetic mutations in the amyloid precursor protein (APP) gene have been described that accelerate the disease process and lower the average age of onset by decades, further supporting a fundamental role for this protein in the disease (2–5). Many questions remain about the spatial–temporal sequence of neuropathological events, particularly what factors are responsible for the selective vulnerability of certain brain regions to amyloidosis. Candidate mechanisms include constitutive increased production of Aβ in vulnerable areas, age-related changes in expression of APP and production of Aβ, and inherent differences in the ability of different brain regions to clear or catabolize Aβ. These fundamental issues are not easily addressed in human subjects.

Similar neuropathology to that seen in human AD brain has been demonstrated in a transgenic mouse generated using a platelet-derived growth factor β promoter driving a human APP minigene (6) and possessing the familial AD mutation V→F at APP position 717 (4) (PDAPP). These animals express high levels of APP and Aβ, but more importantly they exhibit profuse Aβ amyloidosis, which, in an age- and brain region-specific manner, morphologically resembles that seen in AD. In addition, these mice develop marked astrogliosis, microgliosis, cytoskeletal changes, and synaptic loss. They offer the opportunity to examine the biological events leading to amyloidosis and synaptic loss and provide an effective animal model to test for therapeutic agents that have the ability to retard or interfere in these pathological processes.

In this report, we quantitatively assess the profile of a number of APP-derived protein species in different brain regions at various ages in these PDAPP transgenic mice. This is addressed through the use of enzyme-linked immunoassays (ELISAs) configured with antibodies specific to Aβ, $A\beta_{1-42}$, APP cleaved at the β-secretase site (7), and APP containing the first 12 aa of Aβ [i.e., α-secretase-cleaved (8) and full-length (FL) APP]. These biochemical measurements were then compared with the regional distribution of amyloid plaques visualized immunohistochemically. The results suggest that age, Aβ production levels, and brain region-specific factors all likely play critical roles in amyloid deposition in the PDAPP mouse. Striking similarities in both the regional distribution and depositing form of Aβ are noted between the mouse model and the human AD condition. Because of the magnitude and temporal predictability of Aβ deposition, the PDAPP mouse is a practical model in which to test agents that either inhibit the processing of APP to Aβ or retard Aβ amyloidosis.

## MATERIALS AND METHODS

**Transgenic Animals.** The founder of PDAPP line 109 was produced on a Swiss Webster × $B_6D_2F_1$ (C57Bl/6 × DBA/2) background (all strains from Taconic Farms) and bred for three generations with animals of the same background. Generation 3 was bred with $B_6D_2F_1$. Generation 4 was bred with Swiss Webster to produce the outbred heterozygous animals used for these experiments, except where noted. Generation 4 heterozygous animals were bred together to obtain a homozygous animal colony. Generation 4 animals were also bred with C57Bl/6 (The Jackson Laboratory) for five generations to produce a line with a more inbred background. Gross effects on longevity have not been observed in the transgenic lines compared with littermate controls.

**Brain Tissue Preparation.** The heterozygote transgenic (6, 9) and nontransgenic littermate animals were perfused intracardially with ice-cold 0.9% saline. The brain was removed and one hemisphere was prepared for immunohistochemical anal-

The publication costs of this article were defrayed in part by page charge payment. This article must therefore be hereby marked "*advertisement*" in accordance with 18 U.S.C. §1734 solely to indicate this fact.


0027-8424/97/941550-6$2.00/0
PNAS is available online at **http://www.pnas.org**.

Abbreviations: AD, Alzheimer disease; Aβ, amyloid β-peptide; FL, full-length; RT, room temperature.

*To whom reprint requests should be addressed.

ysis, while three brain regions (cerebellum, hippocampus, and cortex) were dissected from the other hemisphere and used for Aβ and APP measurements. For comparative studies of homozygous and heterozygous animals, an additional sample enriched in thalamic matter was dissected.

Tissue for ELISAs was homogenized in 10 volumes of ice-cold guanidine buffer (5.0 M guanidine·HCl/50 mM Tris·Cl, pH 8.0). The homogenates were mixed for 3 to 4 hr at room temperature (RT), then either assayed or stored at −20°C before quantitation of Aβ and APP. Preliminary experiments showed the analytes were stable to this storage condition and that synthetic Aβ peptide (Bachem) could be quantitatively recovered when spiked into littermate control brain tissue homogenates (data not shown).

**Aβ Measurements.** The brain homogenates were further diluted 1:10 with ice-cold casein buffer (0.25% casein/0.05% sodium azide/20 μg/ml aprotinin/5 mM EDTA, pH 8.0/10 μg/ml leupeptin in PBS) before centrifugation (16,000 × *g* for 20 min at 4°C). The Aβ standards (1–40 or 1–42 aa) were prepared such that the final composition included 0.5 M guanidine in the presence of 0.1% bovine serum albumin (BSA).

The "total" Aβ sandwich ELISA consists of the capture antibody 266, which is specific to amino acids 13–28 of Aβ (10), and the biotinylated reporter antibody 3D6, which is specific to amino acids 1–5 of Aβ. The 3D6 antibody does not recognize secreted APP or APP-FL but detects only Aβ species with amino-terminal aspartic acid. The assay has a lower limit of sensitivity of ≈50 pg/ml (11 pM) and showed no crossreactivity to the endogenous murine Aβ peptide at concentrations up to 1 ng/ml (data not shown).

The configuration of the $A\beta_{1-42}$-specific sandwich ELISA employs the capture antibody mAb 21F12 ($A\beta_{33-42}$). Biotinylated 3D6 is also the reporter antibody in this assay, which has a lower limit of sensitivity of ≈125 pg/ml (28 pM; data not shown). An $A\beta_{x-42}$ sandwich ELISA, using 266 as the capture antibody and biotinylated 21F12 as the reporter antibody, was used on a subset of brain homogenates. The low end sensitivity of this assay is ≈250 pg/ml (56 pM; data not shown).

The 266 and 21F12 mAbs were coated at 10 μg/ml into 96-well immunoassay plates (Costar) overnight at RT. The plates were then aspirated and blocked with 0.25% human serum albumin in PBS buffer for at least 1 hr at RT, then stored dessicated at 4°C until use. The plates were rehydrated with wash buffer (0.05% Tween 20 in tris-buffered saline) before use. The samples and standards were added to the plates and incubated at RT for 1 hr. The plates were washed three or more times with wash buffer between each step of the assay.

The biotinylated 3D6, diluted to 0.5 μg/ml in casein assay buffer (0.25% casein/0.05% Tween 20, pH 7.4, in PBS), was incubated in the wells for 1 hr at RT. Avidin–horseradish peroxidase (Vector Laboratories), diluted 1:4000 in casein assay buffer, was added to the wells for 1 hr at RT. The colorimetric substrate, Slow TMB-ELISA (Pierce), was added and allowed to react for 15 min, after which the enzymatic reaction was stopped with addition of 1 M $H_2SO_4$. Reaction product was quantified using a Molecular Devices Vmax spectrophotometer measuring the difference in absorbance at 450 nm and 650 nm.

**APP ELISAs.** Two different APP assays were used (see Fig. 1). The first recognizes APP-α and APP-FL, while the second recognizes APP-β [APP ending at the methionine preceding the Aβ domain (7)]. The capture antibody for both the APP-α/FL and APP-β assays is 8E5 (6). The reporter mAb (2H3) for the APP-α/FL assay was generated against amino acids 1–12 of Aβ. The lower limit of sensitivity for the 8E5/2H3 assay is ≈11 ng/ml (150 pM). For the APP-β assay, the polyclonal antibody 192, specific to the carboxyl terminus of the β-secretase cleavage site of APP (7), was used as the reporter. The lower limit of sensitivity of the 8E5/192 assay is ≈43 ng/ml (600 pM).

For both APP assays, the 8E5 mAb was coated onto 96-well Costar plates as described above for 266. Purified recombinant secreted APP-α (the secreted form of APP 751) and APP596 of the 695 form were the reference standards used for the APP-α/FL and APP-β assays, respectively (8). The 5 M guanidine brain homogenate samples were diluted 1:10 in specimen diluent for a final buffer composition of 0.5 M NaCl, 0.1% Nonidet P-40, and 0.5 M guanidine. The APP standards and samples were added to the plate and incubated for 1.5 hr at RT. Biotinylated reporter antibodies 2H3 and 192 were incubated with samples for 1 hr at RT. Streptavidin–alkaline phosphatase (Boehringer Mannheim), diluted 1:1000 in specimen diluent, was incubated in the wells for 1 hr at RT. The fluorescent substrate 4-methyl-umbellipheryl-phosphate, was added, and the plates were read on a Cytofluor 2350 (Millipore) at 365 nm excitation and 450 nm emission.

**mAb Production.** The immunogens for 3D6 ($A\beta_{1-5}$), 2H3 ($A\beta_{1-12}$), 2G3 ($A\beta_{33-40}$), 21F12 ($A\beta_{33-42}$), and 12H7 ($A\beta_{33-42}$) were separately conjugated to sheep anti-mouse immunoglobulin (Jackson ImmunoResearch). Mice were immunized and hybridomas were generated by standard methods. The hybridoma supernatants were screened for high-affinity mAbs by RIA as previously described (10).

Antibodies 12H7 and 21F12 were demonstrated to show negligible crossreactivity (<0.4%) with $A\beta_{1-40}$ in either ELISA or competitive RIA. Antibody 2G3 was similarly shown to be nonreactive with $A\beta_{1-42}$.

**Immunohistochemistry.** The tissue from one brain hemisphere of each mouse was drop-fixed in 4% paraformaldehyde and postfixed for 3 days. The tissue was mounted coronally and 40-μm sections were collected using a vibratome. The sections were stored in antifreeze solution (30% glycerol/30% ethylene glycol in 40 mM NaPO4) at −20°C before immunostaining. Every sixth section, from the posterior cortex through the hippocampus, was incubated with the appropriate biotinylated antibody (either 3D6, 2G3, or 12H7) at 4°C, overnight. The sections were then reacted with the horseradish peroxidase–avidin–biotin complex (Vector Laboratories) and developed using 3,3′-diaminobenzidine (DAB) as the chromagen.

## RESULTS

**Aβ and APP Assays.** Fig. 1 illustrates the recognition sites of antibodies used in the Aβ and APP assays. The APP-α/FL assay recognizes secreted APP including the first 12 aa of Aβ. Since the reporter antibody (2H3) is not specific to the α-clip site, occurring between Aβ amino acids 16 and 17 (8), this assay also recognizes APP-FL. Preliminary experiments using immobilized APP antibodies to the cytoplasmic tail of APP-FL to deplete brain homogenates of APP-FL suggest that ≈30–40% of the APP-α/FL APP is APP-FL (data not shown). Due to the specificity of the polyclonal reporter antibody, the APP-β assay recognizes only the APP clipped immediately amino-terminal to Aβ (7).

Aβ immunoreactivity was characterized by size exclusion chromatography (Superose 12, Pharmacia) of brain homogenates. Comparisons were made of 2-, 4-, and 12-month-old transgenic brain specimens as well as a 12-month-old nontransgenic mouse brain homogenate to which $A\beta_{1-40}$ had been spiked at a level roughly equal to that found in the 12-month-old transgenic mice. The elution profiles of the transgenic brain homogenates were similar in that the peak fractions of Aβ immunoreactivity occurred in the same position, a single broad symmetric peak that was coincident with the immunoreactive peak of spiked $A\beta_{1-40}$. Attempts were then made to immunodeplete the Aβ immunoreactivity using resin-bound antibodies against Aβ (mAb 266 against $A\beta_{13-28}$), the secreted forms of APP (mAb 8E5 against $APP_{444-592}$ of the 695 form),

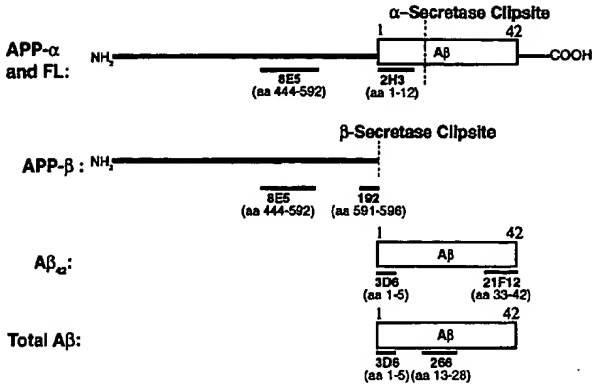


FIG. 1. Immunoassays to forms of Aβ and APP described in the text. Immunoassays were prepared to measure APP-α/FL, APP-β (secreted APP ending at the methionine preceding the start of the Aβ region), and total Aβ. Antibodies are mouse mAbs except 192, which is an affinity-purified rabbit polyclonal antibody. Antibodies 192 and 21F12 are specific to fragments of APP and Aβ, respectively, with carboxyl termini as indicated. Antibody 3D6 is specific for $A\beta_{1-5}$ and does not cross react with APP-α/FL. Methodologies used for the immunoassays are described in text.

the carboxyl terminus of APP (mAb 13G8 $APP_{676-695}$ of the 695 form), or heparin agarose. Only the 266 resin captured Aβ immunoreactivity (data not shown), demonstrating that APP-FL or carboxyl-terminal fragments of APP are not contributing to the Aβ measurement. The $A\beta_{42}$ ELISA uses a capture antibody that recognizes $A\beta_{42}$ but not $A\beta_{1-40}$ peptide. The $A\beta_{42}$ assay, like the total Aβ assay, is not affected by the FL or carboxyl-terminal forms of APP containing Aβ in the homogenates as shown by similar immunodepletion studies (data not shown).

**Total Aβ and APP Measurements.** Fig. 2 shows the levels of total Aβ, APP-α/FL, and APP-β in the hippocampus, cortex, and cerebellum of transgenic mice as a function of age. Each data point represents the mean value for each age group. The relative levels of APP-α/FL and APP-β in all three brain regions remain relatively constant over time. The hippocampus expresses the highest levels of both APP-α/FL and APP-β followed by the cortex and cerebellum, respectively. The mean ± SD values of all ages for APP-α/FL and APP-β levels in the hippocampus are 720 ± 135 pmol/g and 171 ± 17 pmol/g, respectively. In the hippocampus, the levels of APP-α/FL are approximately 3.5- to 6.0-fold higher than that of APP-β at all ages. Since APP-α/FL is 30–40% APP-FL (see above), we estimate the pool of brain APP to consist of ≈50% APP-α, 30% APP-FL, and 20% APP-β.

Since there was a 1.6-fold increase of APP-α/FL in the hippocampus, which displays robust pathology, versus that of the comparatively unaffected cerebellum, we wanted to determine whether this modest increase of transgenic APP expression was the determinant of the regional pathology displayed in this transgenic line. Western blot analysis of APP transgene expression was performed on brain regions from either heterozygous or homozygous transgenic mice (Fig. 3), both of which show the same regional distribution of pathology (data not shown). There are higher levels of APP expression in the thalamus of the homozygous animal than in the hippocampus of the heterozygous animal; yet pathology in the hippocampus of heterozygotes is extensive with early onset, and the thalamus only displays a minor amount of pathology at later ages. Likewise, there are higher levels of transgene expression in the cerebellum of the homozygous animal, a largely unaffected region, than in the cortex of the heterozygous animal, a region with robust pathology. The same type of comparative analysis was performed on Aβ levels, determined by ELISA, in various brain regions of 2-month-old heterozygous and homozygous transgenic animals (Fig. 3). Although higher levels of Aβ are present in the susceptible brain regions than in unaffected regions in the heterozygotes, the Aβ levels in the thalamus of the homozygotes, which show only minimal pathology in older animals, is equivalent to that in the cortex of the heterozygotes, a region displaying robust pathology at an early age.

In contrast to APP levels, Aβ levels increase dramatically with age in the hippocampus and cortex, with the greatest increase in the hippocampus. No such increase was noted in the cerebellum of the PDAPP transgenic mice (Fig. 2). These region-specific increases of Aβ correlate with the 3D6 immunohistochemical results (Fig. 4 and below). Compared with the levels of 4-month-old mice, Aβ levels increase 8-fold by 8 months of age and 400-fold at 18 months of age in cortex (6330 ± 2310 pmol of Aβ per g of tissue at age 18 months). The corresponding increases in Aβ observed in hippocampus are even more impressive, as the 8-month value is 17 times that at 4 months and increases to 500-fold at 18 months of age (20,800 ± 5250 pmol of Aβ per g of tissue at 18 months).

**$A\beta_{42}$ Measurements in Transgenic Mouse Brain.** We next determined if, as in human AD subjects (11, 12), the depositing Aβ is the longer $A\beta_{1-42}$ form by measuring the levels of $A\beta_{1-42}$ in the hippocampus and cortex of transgenic mice at different ages. As shown in Table 1, the increase in Aβ observed with age in the hippocampus and cortex of transgenic mice is due

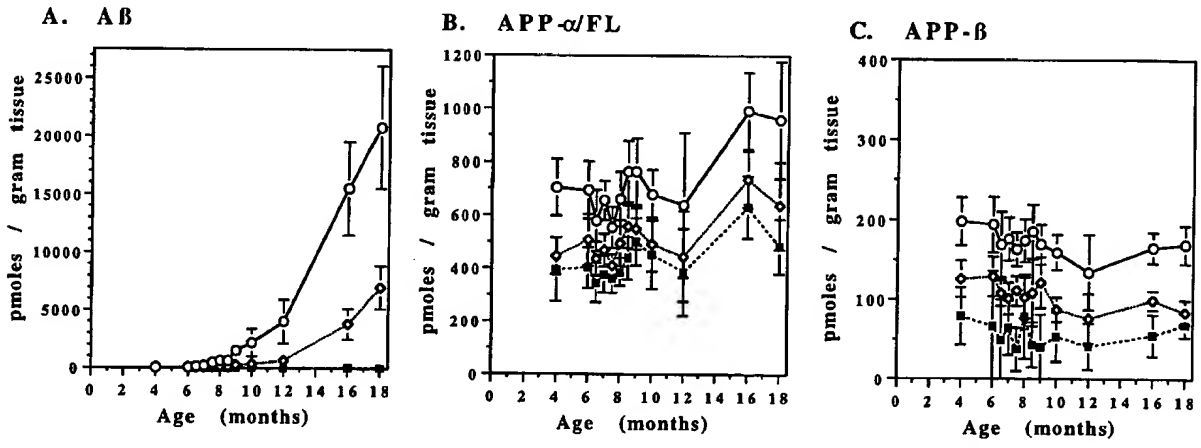


FIG. 2. Age-dependent changes in brain Aβ and APP levels in the PDAPP transgenic mice. PDAPP mice were sacrificed at the ages indicated and levels of Aβ (*A*), APP-β (*B*), and APP-α/FL (*C*) were determined in the cortex (◇), hippocampus (○), and cerebellum (■) by ELISA. Values represent the means ± SD of 9–14 animals.

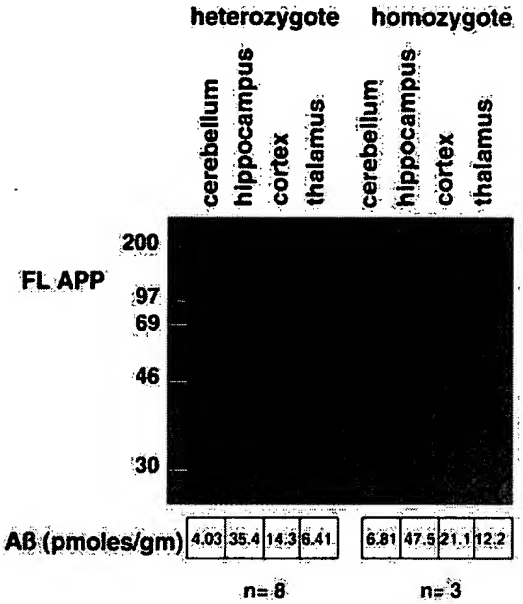


FIG. 3. Levels of APP and Aβ in brain regions of heterozygous and homozygous PDAPP transgenic mice. Two-month-old PDAPP mice were sacrificed, and the amount of APP-FL was measured by Western blot analysis using an APP carboxyl-terminal antibody (anti-6; ref. 6) in hippocampus, cortex, cerebellum, and thalamus of heterozygous and homozygous mice. Essentially similar results were obtained from Western blot analyses using other APP antibodies (human-specific 8E5 and 2H3; data not shown). The amount of Aβ in these same regions from eight heterozygous and three homozygous 2-month-old animals was determined by ELISA, and the average levels are listed.

to $A\beta_{1-42}$. $A\beta_{1-42}$ constituted 27% of the 17 pmol/g of the Aβ present in the brains of young animals, this percentage increased to 89% of the 694 pmol/g in 12-month-old animals. Since the $A\beta_{1-42}$-specific assay does not detect $A\beta_{42}$ with a truncated or modified amino terminus, further analysis of the $A\beta_{42}$ species in the transgenic mice was performed. A subset ($n$ = 4) of 12-month-old PDAPP transgenic mice cortical homogenates were quantitated in the sandwich ELISA measuring $A\beta_{x-42}$ as well as the $A\beta_{1-42}$-specific assay. Approximately 90% of the $A\beta_{42}$ is true $A\beta_{1-42}$ and the remaining 10% begins somewhere other than the amino-terminal aspartic acid of Aβ.

**Aβ Measurements in Outbred and Inbred Strains of PDAPP Transgenic Mice.** The levels of total Aβ in the hippocampus and cortex were compared between the outbred ($n$ = 14) and inbred strains ($n$ = 20) of PDAPP mice at 4 months of age and found to be 15.95 ± 2.70 and 15.51 ± 1.72 pmol/g of tissue in the cortical homogenates and 38.08 ± 6.76 and 33.02 ± 4.56 pmol/g of tissue in the hippocampal homogenates, respectively. Statistical analysis of the cortical and hippocampal Aβ measurements determined that there was not a significant difference in the interanimal variability between the two groups (data not shown).

**Aβ Immunohistochemistry in PDAPP Transgenic Brain.** To correlate Aβ accumulation in brain as measured by ELISA with the deposition of Aβ into plaques as measured immunohistochemically, opposite hemispheres were sectioned and immunoreacted with 3D6. Fig. 4 illustrates the progression of Aβ deposition in 4-, 8-, 10-, 12-, 16-, and 18-month-old animals, with Aβ measurements representative of the mean value of their age group. At 4 months of age, transgenic brains contain small, rare, punctate deposits, ≈20 μm in diameter, that were only infrequently observed in the hippocampus as well as the frontal and cingulate cortex. By 8 months of age, these regions contain a number of thioflavin-positive Aβ aggregates (data not shown) that form plaques as large as 150 μm in diameter. At 10 months of age, many large Aβ deposits are found throughout the frontal and cingulate cortex and the molecular layers of the hippocampus. The outer molecular layer of the dentate gyrus receiving perforant pathway afferents from the entorhinal cortex is clearly heavily delineated by Aβ deposition. This general pattern was more pronounced by heavier Aβ deposition at 1 year of age, and by 18 months of age it involves most of the neocortex. Notably, a striking increase in Aβ plaque burden paralleled the rising Aβ levels (compare Figs. 2*A* and 4). Staining of sections with antibodies specific for $A\beta_{42}$ (Fig. 5*A*) and $A\beta_{40}$ (Fig. 5*B*) indicates that amyloid plaques are primarily composed of $A\beta_{42}$, again paralleling the ELISA results. These findings strongly argue that the rise in brain $A\beta_{42}$ concentration determined by ELISA is due to the age-dependent amyloidosis.

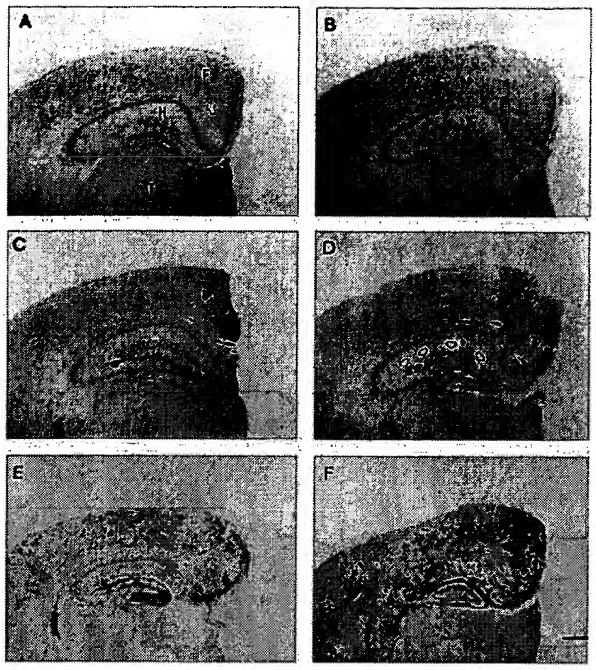


FIG. 4. Age-dependent increases in Aβ plaque burden in the PDAPP mouse. Aβ deposits in the opposite hemisphere of brains used for Aβ and APP ELISAs at 4 (*A*, arrow indicates deposit), 8 (*B*), 10 (*C*), 12 (*D*), 16 (*E*), and 18 (*F*) months of age. Brains are shown from mice with Aβ ELISA values that correspond to the mean of their age group. Deposition typically occurs in an age- and region-dependent manner, with early and heavy involvement of the frontal cortex (F) and hippocampus (H), while the underlying thalamus (T) is devoid of plaques. Arrows in *D* outline the outer molecular layer of the dentate gyrus, which contains terminals from the perforant pathway. [Bar (in *F*) = 500 μm.]

Table 1. Aß levels in the cortex of transgenic brain (pmol of Aß per g of wet tissue)

| Age, months | $n$ | $A\beta_{1-42}$ | Total Aß | % $A\beta_{42}$ |
|---|---|---|---|---|
| 4 | 11 | 4.7 ± 1.3 | 17 ± 3.4 | 27 |
| 8 | 13 | 76 ± 40 | 112 ± 64 | 68 |
| 10 | 5 | 247 ± 133 | 248 ± 139 | 99 |
| 12 | 9 | 615 ± 333 | 694 ± 403 | 89 |
| 16 | 10 | 3538 ± 1104 | 3813 ± 1327 | 93 |
| 18 | 10 | 5612 ± 1583 | 6332 ± 2310 | 89 |

Values are in mean ± SD.

## DISCUSSION

Aβ amyloidosis is an established diagnostic criteria of AD (13, 14) and is consistently seen in higher-order cortical areas as well as the hippocampal formation of the brain in affected subjects. It is believed that Aβ amyloidosis is a relatively early event in the pathogenesis of AD that subsequently leads to neuronal dysfunction and dementia through a complex cascade of events (15, 16). For unknown reasons, other brain regions, such as the cerebellum, are typically spared from advanced forms of amyloidosis in AD. Both the sequence of events of this process as well as the brain region specificity of AD pathology have been extraordinarily difficult to unravel because brain tissue cannot typically be analyzed until after the death of these patients. Recently, reliable and robust Aβ amyloidosis accompanied by neuropathology has been demonstrated in the PDAPP mouse (6), providing a model in which to study these issues. In this report we have investigated the key metabolites of APP as a function of age and anatomical location and compared this to the immunohistochemically detected changes of Aβ in these animals.

Various pathways of APP processing have been described, including the α-secretase pathway in which cleavage of APP occurs within Aβ (Fig. 1 and ref. 8) and the amyloidogenic or β-secretase pathway in which cleavage of APP occurs at the amino terminus of Aβ (Fig. 1 and ref. 7). Further cleavage of APP leads to the constitutive production of Aβ, including the form ending at position 42 ($A\beta_{42}$). We have taken advantage of site-specific antibodies to develop ELISAs that detect specific APP products arising from these individual pathways in the PDAPP mouse brain.

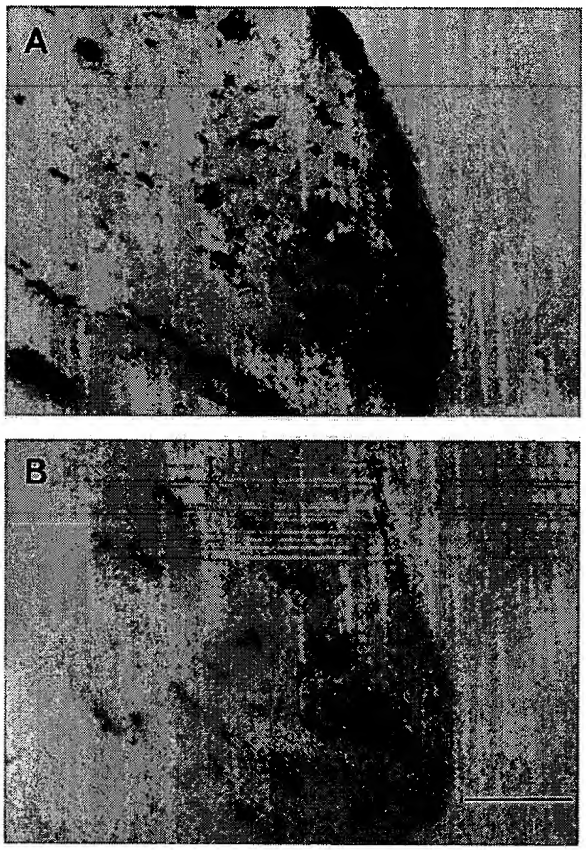


FIG. 5. $A\beta_{42}$ and $A\beta_{40}$ immunohistochemical analysis in 18-month-old PDAPP mice. Aβ deposits in adjacent sections from an 18-month-old mouse visualized with antibodies specific for $A\beta_{42}$ (*A*) and $A\beta_{40}$ (*B*). [Bar (in *B*) = 100 μm.]

Analysis of Aβ and APP immunoreactivities in the PDAPP mouse brain leads to several interesting conclusions. First, levels of APP-α/FL were relatively constant over the age of the PDAPP mice examined and varied only modestly (1.6-fold) among the brain regions analyzed (Fig. 2), indicating that age- or region-dependent changes in expression of the transgene are not amyloidogenic factors in this animal. The lack of amyloid deposition and pathology in the unaffected brain regions in the presence of high levels of APP expression strongly argues that APP overexpression alone is insufficient to cause amyloid deposition in this model. An additional finding that supports this observation is that mice homozygotic for the PDAPP minigene have thalamic levels of APP that exceed those seen in the hippocampus of the heterozygote animals and yet still do not display Aβ deposition in this region (Fig. 3).

To test if region- or age-dependent differential processing of APP to Aβ contributes to Aβ deposition in the PDAPP mouse, we measured the β-secretase product of APP-FL (APP-β) at various ages in different brain regions (7). APP-β is a direct product of β-secretase activity, and its production parallels the production of Aβ *in vitro* under conditions that are expected to either directly modulate the activity of β-secretase or to modulate the accessibility of APP to β-secretase (17–19). Levels of APP-β are therefore thought to correlate with the production of Aβ. The PDAPP mouse thus affords the unique opportunity to measure levels of this metabolite in a tissue destined to undergo amyloidosis at different stages of deposition. Examination of APP-β levels in different brain regions of the PDAPP mouse shows that levels of this APP metabolite do not change significantly with age (Fig. 2). This is true even in the hippocampus where very significant Aβ levels and deposition occur at 8 months of age or greater (Figs. 2 and 4). This finding argues strongly that the age-related amyloid deposition seen in the PDAPP mice is not due to age-dependent increased processing of APP to Aβ mediated by the β-secretory pathway.

Vulnerable brain regions do seem to intrinsically process more APP to Aβ, however. The initial Aβ levels in brains of young animals, before amyloidotic deposition, are higher in hippocampus and cortex than in cerebellum (38.1 pmol/g Aβ in hippocampus, 4.1 pmol/g Aβ in the cerebellum). Levels of APP-β are also higher in amyloid-depositing brain regions; they are 3-fold higher in hippocampus and 2-fold higher in cortex relative to the unaffected cerebellum (Fig. 2). Even normalizing for the 1.5-fold difference in transgenic APP expression between these brain regions, there is 2-fold more APP-β and 7-fold more Aβ in the hippocampus compared with cerebellum, supporting the notion that there is more efficient processing of APP to Aβ in affected brain regions than in unaffected regions. Modest changes in Aβ production, such as in Down syndrome, are sufficient to accelerate amyloid deposition (15). Taken together, these data suggest that increased constitutive processing to Aβ, via the β-secretase pathway, is a significant factor in the brain region specific deposition of Aβ that is seen in the PDAPP mouse.

However, there must be other significant factors in addition to enhanced Aβ production that lead to amyloidosis, since measurements of Aβ or APP-β levels in unaffected brain regions of mice homozygotic for the PDAPP minigene are essentially equivalent to those seen in affected brain regions of the heterozygote PDAPP mice (Fig. 3). This clearly indicates that not only is reaching a threshold level of Aβ required to cause amyloid deposition, but that other regional specific factors are required to interact with Aβ to elicit amyloid deposition. One can only speculate that such factors might include age-dependent expression of specific proteoglycans (20) or specific receptors and binding substances for Aβ such as C1q, Apo E, or APO J (21–23). Such factors may interact with the Aβ peptide and result in its increased aggregation or

fibril formation. The defined regional and time course of amyloid deposition events in this model allow a means to define these factors.

Initial brain levels of Aβ show interanimal variability up to 2-fold. There are no outlying animals with excessively high or absent Aβ. Since the genetic strain of mice can have an effect on transgene phenotype and this line was derived in a highly outbred background, we tested whether the variability could be reduced by crossing it onto an inbred strain. Variability among animals of initial brain Aβ levels does not seem to be due to the genetic variability of the outbred strain since inbred animals displayed the same variability in Aβ as the outbred animals.

Aβ amyloid deposition seen in the PDAPP mouse brain is highly age- and region-specific (Figs. 2 and 4). Amyloid deposition accelerates at around 7 months of age, and by 12 months of age, amyloid deposition is pronounced throughout the hippocampus and in the frontal region of the cortex. Between 12 and 16 months of age, a further dramatic increase in deposition is observed. This anatomical localization of Aβ deposition is remarkably similar to that seen in AD (13). The age-dependent increases in immunohistochemically detectable amyloid deposition correlate well with the dramatic rise in Aβ levels in these brain regions as measured by ELISA. An increase in Aβ is measurable by 7 months of age and by 10 months the hippocampus has 2180 pmol Aβ/g of tissue. By 18 months of age, the levels of $A\beta_{42}$ are comparable to the higher Aβ levels observed in humans with AD (24). Aβ levels in the cerebellum at 10 months, an unaffected brain region, remain at 4 pmol/g of tissue—essentially unchanged relative to the levels at 4 months of age, in agreement with the extent of amyloid deposition observed by histological analyses. Thus, a reproducible increase in measurable Aβ occurs in the brain tissue of the PDAPP mice that correlates with the severity of amyloid deposition. These results suggest that in aged PDAPP mice, monitoring of brain Aβ levels reflects amyloid burden and therefore direct immunoassay measurement of brain Aβ levels can be used to monitor the effects of compounds that reduce amyloid plaque burden.

The vast majority of depositing Aβ in these mice is of the longer $A\beta_{42}$ form, despite the fact that the majority of Aβ produced in younger animals are shorter species (Table 1). The ELISA data suggest that $A\beta_{42}$ is preferentially depositing in the transgenic mice, a result confirmed by immunostaining (Fig. 5). This is in agreement with studies of human AD and of Down syndrome brains, wherein the predominant and initially depositing Aβ is the longer form (11). In this respect, this mouse model again faithfully reproduces human AD pathology, indicating that the biological mechanisms leading to the preferential deposition of $A\beta_{42}$ in AD are conserved in the mouse. At 18 months of age, the percentage of shorter Aβ is essentially the same as at 12 months in both the cortex and hippocampus. Immunohistochemistry suggests that deposition of the $A\beta_{40}$ species is primarily in compacted plaques, as opposed to increasing amyloid angiopathy. The fact that the majority of Aβ detected in the mouse begins at Asp-1 is different from that reported in human AD (24). However, it is not clear how much of the amino-terminal modification in the human occurs after deposition. In AD, the plaques presumably have a residence time of several years, in contrast to several months, as in the case of the PDAPP mouse. The $A\beta_{42}$ found in the cerebrospinal fluid of AD patients is primarily $A\beta_{1-42}$ (unpublished data), suggesting the predominant cleavage sites are not shifted in the mouse from that in AD.

Aside from the insights into Aβ amyloidosis offered by the PDAPP model, there is a practical use of these studies as well. Using these measurements, it is now feasible to test agents that reduce Aβ peptide burden by preventing its production. Compounds designed to prevent or reverse Aβ deposition can also be evaluated in a reasonable *in vivo* fashion. Such agents, designed to prevent or reduce amyloidosis and plaque burden, will afford a new approach to the treatment of AD.


1. Selkoe, D. (1994) *Annu. Rev. Neurosci.* **17,** 489–517.
2. Goate, A., Chartier-Harlin, M.-C., Mullan, M., Brown, J., Crawford, F., *et al.* (1991) *Nature (London)* **349,** 704–706.
3. Chartier-Harlin, M.-C., Crawford, F., Houlden, H., Warren, A., Hughes, D., Fidani, L., Goate, A., Rossor, M., Roques, P., Hardy, J. & Mullan, M. (1991) *Nature (London)* **353,** 844–846.
4. Murrell, J., Farlow, M., Ghetti, B. & Benson, M. (1991) *Science* **254,** 97–99.
5. Mullan, M., Crawford, F., Axelman, K., Houlden, H., Lilies, L., Winblad, B. & Lannfelt, L. (1992) *Nat. Genet.* **1,** 345–347.
6. Games, D., Adams, D., Alessandrini, R., Barbour, R., Berthelette, P., *et al.* (1995) *Nature (London)* **373,** 523–527.
7. Seubert, P., Oltersdorf, T., Lee, M., Barbour, R., Blomquist, C., Davis, D., Bryant, K., Fritz, L., Galasko, D., Thal, L., Lieberburg, I. & Schenk, D. (1993) *Nature (London)* **361,** 260–263.
8. Esch, F., Keim, P., Beattie, E., Blacher, R., Culwell, A., Oltersdorf, T., McClure, D. & Ward, P. (1990) *Science* **248,** 1122–1124.
9. Rockenstein, E., McConlogue, L., Tan, H., Power, M., Masliah, E. & Mucke, L. (1995) *J. Biol. Chem.* **270,** 28257–28267.
10. Seubert, P., Vigo-Pelfrey, C., Esch, F., Lee, M., Dovey, H., Davis, D., Sinha, S., Schlossmacher, M., Whaley, J., Swindlehurst, C., McCormack, R., Wolfert, R., Selkoe, D., Lieberburg, I. & Schenk, D. (1992) *Nature (London)* **359,** 325–327.
11. Iwatsubo, T., Odaka, A., Suzuki, N., Mizusawa, H., Nukina, N. & Ihara, Y. (1994) *Neuron* **13,** 45–53.
12. Roher, A., Lowenson, J., Clarke, S., Wolkow, C., Wang, R., Cotter, R., Reardon, I., Zurcher-Neely, H., Heinrikson, R., Ball, M. & Greenberg, B. (1993) *J. Biol. Chem.* **268,** 3072–3083.
13. Mirra, S., Heyman, A., McKeel, D., Sumi, S., Crain, B., Brownlee, L., Vogel, F., Hughes, J., van Belle, G., Berg, L. & participating Consortium to Establish a Registry for Alzheimer's Disease (CERAD) neuropathologists (1991) *Neurology* **41,** 479–486.
14. Khachaturian, Z. (1985) *Arch. Neurol. (Chicago)* **42,** 1097–1105.
15. Mann, D., Yuonis, N., Jones, D. & Stoddart, R. W. (1992) *Neurodegeneration* **1,** 201–215.
16. Morris, J., Storandt, M., McKeel, D., Rubin, E., Price, J., Grant, E. & Berg, L. (1996) *Neurology* **46,** 707–719.
17. Citron, M., Oltersdorf, T., Haass, C., McConlogue, L., Hung, A., Seubert, P., Vigo-Pelfrey, C., Lieberburg, I. & Selkoe, D. (1992) *Nature (London)* **360,** 672–674.
18. Cai, X.-D., Golde, T. & Younkin, S. (1993) *Science* **259,** 514–516.
19. Knops, J., Suomensaari, S., Lee, M., McConlogue, L., Seubert, P. & Sinha, S. (1995) *J. Biol. Chem.* **270,** 2419–2422.
20. Snow, A., Sekiguchi, R., Nochlin, D., Fraser, P., Kimata, K., Mizutani, A., Arai, M., Schreier, W. & Morgan, D. (1994) *Neuron* **12,** 219–234.
21. Rogers, J., Cooper, N., Webster, S., Schultz, J., McGeer, P., Styren, S., Civin, W., Brachova, L., Bradt, B., Ward, P. & Lieberburg, I. (1992) *Proc. Natl. Acad. Sci. USA* **89,** 10016–10020.
22. Strittmatter, W., Saunders, A., Schmechel, D., Pericak-Vance, M., Enghild, J., Salvesen, G. & Roses, A. (1993) *Proc. Natl. Acad. Sci. USA* **90,** 1977–1981.
23. Ghiso, J., Matsubara, E., Koudinov, A., Choi-Miura, N., Tomita, M., Wisniewski, T. & Frangione, B. (1993) *Biochem. J.* **293,** 27–30.
24. Gravina, S., Ho, L., Eckman, C., Long, K., Otvos, L., Younkin, L., Suzuki, N. & Younkin, S. (1995) *J. Biol. Chem.* **270,** 7013–7016.